xx (138680.1)

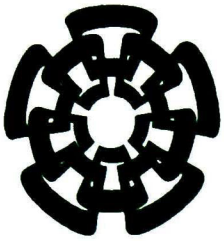

Centro de Investigación y de Estudios Avanzados del I.P.N.
Unidad Guadalajara

Modelado de Líneas de Transmisión Multiconductoras No Uniformes en el Dominio del Tiempo para el estudio de Transitorios Electromagnéticos

Tesis que presenta:
Alejandro Rafael Chávez Bustos

para obtener el grado de:
Doctor en Ciencias

en la especialidad de:
Ingeniería Eléctrica

Director de Tesis:
Dr. Pablo Moreno Villalobos

Guadalajara Jalisco, Octubre 2007.

Modelado de Líneas de Transmisión Multiconductoras No Uniformes en el Dominio del Tiempo para el estudio de Transitorios Electromagnéticos

Tesis de Doctorado en Ciencias
Ingeniería Eléctrica

Por:
Alejandro Rafael Chávez Bustos
Maestro en Ciencias con Especialidad
en Ingeniería Eléctrica
Centro de Investigación y de Estudios Avanzados del
Instituto Politécnico Nacional 1999-2001

Becario de CONACYT, expediente no. 143958

Director de Tesis:
Dr. Pablo Moreno Villalobos

CINVESTAV del IPN Unidad Guadalajara, Octubre 2007.

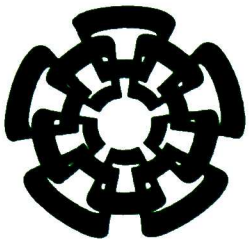

Centro de Investigación y de Estudios Avanzados

del I.P.N.

Unidad Guadalajara

Nonuniform Multiconductor Transmission Lines Modeling for Time Domain Electromagnetic Transient Studies

A thesis presented by:
Alejandro Rafael Chávez Bustos

to obtain the degree of:
Doctor in Science

in the subject of:
Electrical Engineering

Thesis Advisors:
Dr. Pablo Moreno Villalobos

Guadalajara Jalisco, October 2007.

Nonuniform Multiconductor Transmission Lines Modeling for Time Domain Electromagnetic Transient Studies

Doctor of Science Thesis
In Electrical Engineering

By:
Alejandro Rafael Chávez Bustos
Master of Science in Electrical Engineering
Centro de Investigación y de Estudios Avanzados del
Instituto Politécnico Nacional 1999-2001

Scholarship granted by CONACYT, No. 143958

Thesis Advisors:
Dr. Pablo Moreno Villalobos

CINVESTAV del IPN Unidad Guadalajara, October 2007.

RESUMEN

En este trabajo, se presentan dos modelos para el Análisis de Transitorios Electromagnéticos en el dominio del tiempo para líneas de Transmisión Multiconductoras No Uniformes; tomando en cuenta la dependencia frecuencial de sus parámetros eléctricos y además considerando que son excitadas por campos electromagnéticos incidentes.

Uno de los modelos esta basado en un método de diferencias finitas en el dominio del tiempo o método de Yee. Este método tiene la ventaja de fácil entendimiento y no presenta gran dificultad para su programación. Sin embargo, el método de Yee es propenso a oscilaciones numéricas.

El otro modelo que se presenta esta basado en el Método de las Características de la teoría de ecuaciones diferenciales parciales. Este modelo requiere el dominio de la teoría de ecuaciones diferenciales parciales y análisis modal, pero proporciona una solución robusta para el problema de propagación de onda en líneas de transmisión multiconductoras No Uniformes.

Con el objetivo de que el Método de las Características represente un método de análisis práctico, las ecuaciones de las Características de la línea Multiconductora se expresan de una forma que permite definir Circuitos Equivalentes de Norton para los extremos de la línea de transmisión. Estos circuitos equivalentes hacen posible la inclusión del Modelo con el Método de las Características a programas de propósito general o comercial para el análisis de transitorios, tales como el EMTP/ATP.

ABSTRACT

In this work, two models for incident fields excited Nonuniform Multiconductor Transmission lines with frequency dependent parameters for time domain electromagnetic transients analysis are presented.

One of the models is based on the Finite Difference Time Domain method or Yee's method. This method has the advantage that is easy to understand and does not present a heavy programming burden. However it is shown that it is prone to numerical oscillations.

The other model is based on the Method of Characteristics from the partial differential equations theory. This Model requires understanding of some theory of partial differential equations and modal analysis but provides a robust solution for the wave propagation problem in multiconductor transmission lines.

In order to bring the Method of Characteristics to a practical stage; the Characteristics equations for the multiconductor line are cast into a form that permits defining Norton equivalent circuits for the transmission line ends. These equivalent circuits make possible the inclusion of the Characteristics models into a general purposes program for transient analysis, such as EMTP/ATP.

The results obtained with the developed model are compared with those from the EMTP and a Numerical Laplace program.

Acknowledgement

I firstly thank God to let me live and finish this stage of my life.

I would like to thank too, all the support from my family specially to my grandparents José Cruz Chávez Mata †, María Teresa Padilla Hernandez, Rafael Bustos Vives †, Edilta Peraza Pereyra †, and of course to my parents and brothers, José Cruz Chávez Padilla, Lilia Bustos Pereza, José Cruz, Luis Eduardo and Liliana Teresa.

At the same manner I would like to express all my gratitude to Dr. Pablo Moreno Villalobos and Dr. José Luis Naredo for their invaluable guidance during this work, for all their advices and over all their friendship and support.

I thank Dr. Abner Ramirez for his unconditional support and his friendship when I went abroad for my staying at UBC. I also thank Dr. J. R. Marti and Dr. Luis Linares for their instructions, their time and over all their friendship at UBC. To all my Laboratory partners at UBC with whom I cohabited; they help me, support me and gave me all their friendship, for that, I missed my country just a little. I would especially like to thank to Heesang, Leweii and Tom, UBC laboratory friends who always had time to attend me.

In the same way I would like to thank to Olivia Blas Solano and her family who always and unconditionally give me all their support.

I also give thanks to all my Cinvestav-Guadalajara unit friends and partners, I would like to mention each one of them but I would not finish; to everybody that works in the administrative department, especially Lupita Ciprian and all the professors with whom I cohabited or took courses.

Finally, I thank to CONACYT who supplied all the economic issues to get this work.

INDEX

Resumen..... i

Abstract..... ii

Acknowledgment..... iii

Index..... iv

List of figures..... vi

1. Introduction
   1.1 Problem Approach..... 1
   1.2 Background..... 1
   1.3 Objective..... 4

2. Nonuniform Multiconductor transmission lines with frequency dependent parameters
   2.1 Introduction..... 5
   2.2 Multiconductor Transmission Lines Equations with frequency dependent electrical parameters..... 6
   2.3 Method of Characteristics..... 9
   2.4 Recursive Convolution..... 12
   2.5 Numerical Solution..... 13
   2.6 Iterative Procedure..... 15
   2.7 Boundary Conditions..... 16
   2.8 Application Example..... 19
   2.9 Observations..... 22

3. Piecewise Uniform Model for Nonuniform Multiconductor Transmission Lines
   3.1 Introduction..... 24
   3.2 Piecewise Mode..... 24
   3.3 Boundary Conditions..... 27
   3.4 Application Examples..... 29
   3.5 Observations..... 34

4. Finite Difference time domain method for field excited Nonuniform Multiconductor Transmission Lines
4.1 Introduction..... 35
4.2 Nonuniform Multiconductor Transmission Line equation with incident electromagnetic field..... 35
4.3 Yee's Method..... 36
4.4 Boundary Conditions..... 39
4.5 Application Examples..... 41
4.6 Observations..... 45

5. The Method of Characteristics for field excited Nonuniform Multiconductor Transmission
5.1 Introduction..... 46
5.2 Method of Characteristics..... 46
5.3 Numerical Solution..... 49
5.4 Boundary Conditions..... 51
5.5 Application Examples..... 53
5.6 Observations..... 56

6. Conclusions and Future work
6.1 Conclusions 57
6.2 Future Work 58

References..... 59

Published Work..... 63

LIST OF FIGURES

Fig.2.1. Characteristics in the x-t plane..... 14

Fig.2.2. Characteristics curves at the sending end of the transmission line..... 17

Fig.2.3. Characteristics curves at the receiving end of the transmission line... 18

Fig.2.4. Norton equivalent circuit for the transmission line's ends..... 19

Fig.2.5. Nonuniform Transmission Line geometry..... 20

Fig.2.6. Waveform at the Phase C of the receiving node of a nonuniform three-phase line: NLTP and Method of Characteristics..... 20

Fig.2.7. Waveform at the phase C of the receiving node of a uniform three-phase line: EMTP and Method of Characteristics..... 21

Fig. 2.8. Waveforms using a different set of poles for each line segment and using the same set of poles for all the line segments..... 22

Fig. 3.1. Characteristics in the *x-t* plane 26

Fig.3.2. Characteristic at the sending end of the line 28

Fig.3.3. Characteristics at the receiving end of the line..... 28

Fig.3.4. Nonuniform Transmission Line geometry..... 30

Fig.3.5. Waveform at the Phase C of the receiving node of a nonuniform three-phase line: NLTP and Method of Characteristics..... 30

Fig.3.6. Waveform at the Phase C of the receiving node of a nonuniform three-phase line: NLTP and Piecewise Uniform form 31

Fig.3.7. Waveform at the Phase C of the receiving node of a nonuniform three-phase line: EMTP and NLTP..... 31

Fig.3.8. Vertical Multiconductor Transmission Line System 32

Fig.3.9. Current Source injected at the top of the vertical transmission lines System..... 33

Fig.3.10. Voltages at the top of the Vertical Multiconductor Transmission Line System..... 33

Fig.4.1. FD-TD grid..... 38

Fig.4.2. Voltages and current at the sending end for the grid of Yee's method 39

Fig.4.3. Voltages and current at the receiving end Yee's mesh 40

Fig.4.4. Norton equivalent circuit for the transmission line ends based on Yee's Method..... 41

Fig.4.5. Nonuniform Transmission Line geometry..... 42

Fig.4.6. Waveform voltages at the receiving end phase C. EMTP against Method of Yee..... 42

Fig.4.7. Nonuniform three phase Transmission Line geometry 43

Fig.4.8. Incident Electric Field..... 44

Fig.4.9. Incident Magnetic Field..... 44

Fig.4.10. Waveforms Voltage at the sending end phase C. EMTP against Method of Yee..... 45

Fig.5.1. Characteristics in the x-t plane..... 49

Fig.5.2. Characteristics curves at the sending end of the transmission line..... 51

Fig.5.3. Characteristics curves at the receiving end of the transmission line... 52

Fig.5.4. Norton equivalent circuits for the transmission line ends taking into account the electric and magnetic external fields..... 52

Fig.5.5. Nonuniform Line geometry..... 53

Fig.5.6. Electric field waveform..... 54

Fig.5.7. Magnetic field waveform..... 54

Fig.5.8. Voltages waveform at the sending end (and receiving end) with the Method of Characteristics and Yee's Method..... 55

Fig.5.9. Voltage waveforms at the sending end (and receiving end) for the EMTP and the Method of Characteristics..... 56

1 INTRODUCTION

1.1 PROBLEM APPROACH

In the analysis of electromagnetic transients of electric power systems, the interest on studies of elements whose electric parameters change with respect to the spatial variables has increased. Examples of these elements are transmission lines, transmission towers, transformers and electrical machines. In spite of the fact that lines show progressive variations in their parameters, they are generally supposed as uniform or as a serial chain of uniform lines connected by cascade. This approach provides acceptable results for several transient phenomena. However, when dealing with fast electromagnetic transient studies, as in the case of overvoltages created by lightning, it could be necessary to take into account the gradual variation of the electric parameters.

Regarding transmission lines, besides the variation of the electrical parameters along their length, there exist other problems of practical interest. Examples of these problems are the frequency dependence of the electric parameters and the effects of electromagnetic fields generated by lightning, radiating structures or transmitting antennas.

1.2 BACKGROUND

During the last 50 years a number of models for electromagnetic transient studies on transmission lines whose parameters change with the distance, so called Nonuniform lines, have been developed.

In 1954, C. F. Wagner, I. W. Gross and B. L. Lloyd, presented one of the first articles that reported experimental measurements on nonuniform three phase transmission lines and transmission towers under different operation conditions [1]. Since then those studies have been used by other researchers in validating results obtained with several models.

One of the first attempts to solve the nonuniform line problem was proposed by C. Menemenlis and Z.T. Chun in 1982 [2]. They modeled the wave propagation on

nonuniform transmission lines using the conventional technique of Lattice Diagrams. This model considers that along the line exist small discontinuities that produce reflections of voltage and current waves and in consequence, introduce a transmission and a reflection coefficient for each point of discontinuity along the line. The principal limitation of this technique is that such coefficients must be real and the line must be lossless. In 1989, A. Ametani and M. Auki, developed expressions to obtain the impedance and admittance of nonuniform and non-parallel conductor systems [3].

In 1990, M. Mostafa Saied, A. S. Alfuhaid and M. E. El. Shandwily, proposed a model in the s domain [4], for electromagnetic transient studies in nonuniform transmission lines. The advantage of the method was the ability to provide solutions at any location along the line.

Latter in 1996, M. T. Correia de Barros and M. E. Almeida, presented a model for single phase nonuniform Transmission Line based on a finite difference algorithm [5]. This model considered losses distributed along the line. However, the frequency dependence of the electrical parameters was not taken into account.

In 1997, H. V. Nguyen, H. W. Dommel and J.R. Marti, developed an exponential model for single phase lines [6]. Starting from a 2 port representation, the frequency dependent functions are synthesized using rational functions. The time domain equations are reduced to a similar form to those used in the Bergeron method and then solved by means of recursive convolutions.

In 1999, A. Semlyen, performed a frequency domain analysis of the propagation functions and the characteristic admittance behavior for different cases of nonuniform multiconductor transmission lines and identified the oscillations due to the non uniformities [7].

In 1999, Gutierrez, *et. al.* used the Method of Characteristics and finite difference schemes to solve the PDE's of a frequency independent single phase NUL [8]. Davila *et. al.* extended this method in 2002 to consider both frequency and space dependence [9].

In 2001, M. S. Mamis and M. Köksal, published a model for nonuniform single phase transmission lines in the s domain [10]. The transmission line was formed by a connection

of chain matrices. They presented several examples of lightning phenomena in transmission towers and ground conductors with sagging.

In the same year, A. I. Ramirez, A. Semlyen and R. Iravani, developed a model for multiconductor transmission lines [11]. The basis for this work was the study published by Semlyen in 1999 [7] and they proposed equivalent "Norton" circuits to model the transmission line.

Regarding transmission lines excited by external electromagnetic fields, in 1976 R. P. Clayton published one the first studies in this area [12]. He presented the coupling equations that take into account the voltages and currents induced on the transmission line by incident electric and magnetic fields in the frequency domain.

Later in 1980, A. K. Agrawal, H. J. Price and S. H. Gurbaxani derived the transmission line equations with electromagnetic coupling from Maxwell's equations in the time domain [13]. They obtained two formulations, one in terms of the scattered voltages and currents and other using the total voltages and currents. They found the solution to the wave propagation problem applying finite differences to the scattered voltages formulation.

In 1995, T. Henriksen proposed a model for analyzing the overvoltages induced by lightning using the EMTP [14]. The model consisted on dividing the line into several segments and locating sources between every pair of transmission line segments. This model did not include the effects of the magnetic field.

Also in 1995, A. Xemard, Ph. Baraton and F. Boutet, developed a model that did not required dividing the transmission line [15]. In this model the coupling with the electromagnetic field was modeled using only two sources at one transmission line end. The disadvantage of this model is that calculating those sources is very cumbersome and the resulting equations could have no analytic solutions.

In the same year, M. D'Amore and M. S. Sarto presented a procedure to calculate the effects of incident electromagnetic fields on multiconductor transmission lines with frequency dependent parameters using the EMTP [16].

1.3 OBJECTIVE

The objective of this work is to develop a Multiconductor Transmission Line model for electromagnetic transient studies in the time domain. This model will solve the three following problems:

- Variation of the electric parameters with respect to the distant or height (Non uniformities).
- Dependence of electric parameters with respect to the frequency (Skin effect).
- Presence of incident electromagnetic fields.

2 NONUNIFORM MULTICONDUCTOR TRANSMISSION LINES WITH FREQUENCY DEPENDENT PARAMETERS

2.1 INTRODUCTION

In the analysis of electromagnetic transients in Electric Power Systems, there is an increasing interest about the study of elements whose electrical parameters change with the distance. These elements can be transmission lines, transmission towers, transformers and electrical machines windings, for example. Generally, when non uniformities exist mean values are assumed. However, for a number of practical cases, such as fast transients analysis, electrical parameters distance variation may have an important effect on transient waveforms. Regarding transmission lines, although they often show progressive variations along their length, in most transient studies they are considered as uniform elements, i.e., with constant cross section and constant electrical properties of conductors and dielectrics. A nonuniform (NU) Transmission Line (TL) can be modeled as a set of uniform segments connected in cascade; the subdivision procedure when using a general-purpose program is cumbersome and lengthy, though. Moreover a great deal of experience is needed in order to define the optimal number of line sections.

Several methods for analyzing NU lines have been proposed. Some are based on frequency domain techniques [4,17] while others are based on time domain techniques [2,5,6].

For the reason of compatibility with the Electromagnetic Transient Program (EMTP), mainly, the latter ones are preferred. In a recent paper by Semlyen, a new development using the ABCD transmission matrix for the analysis of NU Multiconductor TLs has been presented [7]. In this work the key idea is the determination of the frequency domain propagation functions of an equivalent two-port model. In some cases such propagation

functions can be non-smooth and damping techniques for time domain simulations should be used [11].

The Method of Characteristics [18], one of several solution methods that discretize both time and distance, represents another approach to analyze electromagnetic transients in TLs. This method has successfully been used in calculating transients on NU single-phase lines, e.g., overhead horizontal lines with sagging and vertical conductors [19,20]. Moreover, this method has been applied to the simulation of Single-phase Lines with nonlinear effects due to corona [21]. Recently the Method of Characteristics has been used in the analysis of external fields excited Uniform Multiconductor TLs with frequency dependent parameters [22]. It has been reported that this method does not present the numerical oscillations that are very common in other time domain models.

In this work the Method of Characteristics is applied to the transient analysis of NU Multiconductor TLs with frequency dependent parameters. In addition, in order to make the proposed model suitable to be interfaced with programs based in nodal formulation, for instance the EMTP, Norton equivalent models are presented. Non uniformities of overhead TLs can result from changes in height or radius of conductors, or variations of the electrical properties of conductors and terrain. In particular in this work non uniformities due to sagging of conductors are considered as an example. Results obtained with the proposed model are compared with those from the EMTP and a Numerical Laplace Transform Program (NLTP) [23].

2.2 MULTICONDUCTOR TRANSMISSION LINES EQUATIONS WITH FREQUENCY DEPENDENT ELECTRICAL PARAMETERS.

The Electromagnetic behavior of a Multiconductor overhead transmission line with frequency dependent electrical parameters can be described by a modified version of the equations proposed by Radulet, et al [24].

$$\frac{\partial}{\partial x}\mathbf{v}(x,t)+\mathbf{L}_G\frac{\partial}{\partial t}\mathbf{i}(x,t)+\frac{\partial}{\partial t}\int_0^t \mathbf{r}'(t-\tau)\mathbf{i}(x,\tau)d\tau=\mathbf{0} \tag{2.1}$$

$$\frac{\partial}{\partial x}\mathbf{i}(x,t)+\mathbf{C}\frac{\partial}{\partial t}\mathbf{v}(x,t)=\mathbf{0} \tag{2.2}$$

where $\mathbf{v}(x,t)$ and $\mathbf{i}(x,t)$ are the voltage and current vectors, respectively; $\mathbf{L}_G$ an $\mathbf{C}$ are the per-unit-length geometric inductance and capacitance matrices and $\mathbf{r}'(t)$ is the transient resistance matrix. For a system of n conductors with ground return all the matrices are of dimension nxn.

The element $r'_{ij}(t)$ of the transient resistance matrix is defined as the p.u. voltage drop at the periphery of the i-th conductor that appears after the injection of a current unit step $i=u(t)$ at the j-th conductor:

$$r'_{ij}(t) = -\left.\frac{\partial v_i}{\partial x}\right|_{i_j=u(t)} \qquad t>0 \tag{2.3a}$$

The transient resistance is a positive matrix function that fulfills the followings properties:

$$\lim_{t\to\infty} \mathbf{r}'(t) = diag\{\mathbf{R}_{dc}\} \tag{2.3b}$$

and

$$\lim_{t\to 0} \mathbf{r}'(t) = \infty \tag{2.3c}$$

In order to calculate $\mathbf{r}'(t)$, the classic Telegrapher's equations in the frequency domain can be used. The transmission line equation corresponding to the voltage longitudinal drop is

$$-\frac{d\mathbf{V}(x,s)}{dx} = \left[s\mathbf{L}_G + \mathbf{Z}_C(s) + \mathbf{Z}_e(s)\right]\mathbf{I}(x,s) \tag{2.4}$$

where $\mathbf{V}(x,s)$ and $\mathbf{I}(x,s)$ are the voltage and current vectors in the Laplace domain, respectively; $\mathbf{Z}_C(s)$ and $\mathbf{Z}_e(s)$ are the per-unit-length internal and earth return impedance matrices respectively.

If the Laplace transform is applied to (2.1), it can be written:

$$-\frac{d\mathbf{V}(x,s)}{dx} = \left[s\mathbf{L}_G + s\mathbf{R}'(s)\right]\mathbf{I}(x,s) \tag{2.5}$$

where $\mathbf{R}'(s)$ is the transient resistance matrix in the Laplace domain. Comparing (2.5) and (2.4) gives:

$$\mathbf{R}'(s) = \frac{[\mathbf{Z}_e(s) + \mathbf{Z}_C(s)]}{s} \tag{2.6}$$

Analytical expressions for $\mathbf{Z}_e$(s) and $\mathbf{Z}_C$(s) are well known for the case of multiconductor overhead TLs [25,26]. The known expressions for the internal and return path impedances involve irrational functions, this fact makes very difficult finding **r'**(t) from **R'**(s). To overcome this problem **R'**(s) can be calculated over any frequency range and then each one of its elements may be approximated by a rational function expanded in partial fractions as follows [27]:

$$R_{ij} = \frac{1}{s}k_0 + k_\infty + \sum_{l=1}^{N} \frac{1}{s - p_l} k_l \tag{2.7}$$

Synthesizing poles and residues of (2.7) can be readily accomplished resorting to several existing methods [28-31]. When the vector fitting technique is used [31], algebraic procedures and numerical computation can be simplified. Hence using this technique it can be written:

$$\mathbf{R}'(s) \cong \frac{1}{s}\mathbf{K}_0 + \mathbf{K}_\infty + \sum_{l=1}^{N} \frac{1}{s - \mathbf{p}_l} \mathbf{K}_l \tag{2.8}$$

and in the time domain:

$$\mathbf{r}'(t) \cong u(t)\mathbf{K}_0 + \delta(t)\mathbf{K}_\infty + \sum_{i=1}^{N} e^{\mathbf{p}_l} \mathbf{K}_l \tag{2.9}$$

it can be shown that (2.9) satisfy the initial value theorem

$$\lim_{t\to\infty} \mathbf{r}'(t) = \lim_{s\to 0} s\mathbf{R}'(s) = \mathbf{K}_0 \tag{2.10a}$$

and the final value theorem

$$\lim_{t\to 0} \mathbf{r}'(t) = \lim_{s\to\infty} s\mathbf{R}'(s) = \infty \tag{2.10b}$$

According to (2.3) and (2.10) it can be seen that $\mathbf{K}_0$ is the diagonal matrix equal to the direct current resistance $\mathbf{R}_{dc}$ matrix. Therefore the rational fitting problem consists now on synthesizing the following expansion:

$$\mathbf{R}_{syn}(s) = \mathbf{H}(s) + \mathbf{K}_\infty \tag{2.11}$$

where:

$$\mathbf{H}(s) = \sum_{l=1}^{N} \mathbf{K}_l [s + \mathbf{p}_l]^{-1} \tag{2.12}$$

Substituting the time domain form of **r'***(t)* given by (2.9) into (2.1) gives finally:

$$\frac{\partial}{\partial x}\mathbf{v}(x,t) + \mathbf{L}_{cor}\frac{\partial}{\partial t}\mathbf{i}(x,t) + \mathbf{R}_{dc}\mathbf{i}(x,t) + \frac{\partial}{\partial t}\int_0^t \mathbf{h}(t-\tau)\mathbf{i}(x,\tau)d\tau = \mathbf{0} \tag{2.13}$$

where:

$$\mathbf{L}_{cor} = \mathbf{L}_G + \mathbf{K}_\infty \tag{2.14a}$$

$$\mathbf{h}(t) = \sum_{l=1}^{N} e^{\mathbf{p}_l t}\mathbf{K}_l \tag{2.14b}$$

Equations (2.13) and (2.2) describe the electromagnetic behavior of a Multiconductor Overhead TL with frequency dependent electrical parameters.

2.3 METHOD OF CHARACTERISTICS

The Method of Characteristics consists on transforming the Partial Differential Equations (PDEs) of TLs in Ordinary Differential Equations (ODEs); and then solving the resultant ODEs system by means of any suitable method.

For the case of NU Transmission Lines the PDE's (2.13) and (2.2) can compactly be expressed as follows:

$$\frac{\partial}{\partial t}\mathbf{U} + \mathbf{A}\frac{\partial}{\partial x}\mathbf{U} + \mathbf{B}\mathbf{U} + \mathbf{f} = \mathbf{0} \tag{2.15}$$

where:

$$\mathbf{U} = \begin{bmatrix} \mathbf{v}(x,t) \\ \mathbf{i}(x,t) \end{bmatrix} \tag{2.16a}$$

$$\mathbf{A} = \begin{bmatrix} 0 & \mathbf{C}^{-1}(x) \\ \mathbf{L}_{cor}^{-1}(x) & 0 \end{bmatrix} \tag{2.16b}$$

$$\mathbf{B} = \begin{bmatrix} \mathbf{0} & \mathbf{0} \\ \mathbf{0} & \mathbf{L}_{cor}^{-1}(x)\mathbf{R}_{dc}(x) \end{bmatrix} \tag{2.16c}$$

$$\mathbf{f} = \begin{bmatrix} \mathbf{0} \\ \mathbf{L}_{cor}^{-1}(x)\boldsymbol{\xi}(x,t) \end{bmatrix} \tag{2.16d}$$

and

$$\boldsymbol{\xi}(x,t) = \frac{\partial}{\partial t}\left[\int_0^t \mathbf{h}(x,t-\tau)\mathbf{i}(x,\tau)d\tau\right] \tag{2.16e}$$

Expression (2.15) represents a system with 2n first order PDEs with x and t as independent variables. In (2.16) it has been shown the per-unit-length electrical parameters as a function of the distance to emphasize the NU property of the line. In the following the x variable of the electrical parameters will be omitted for the sake of simplicity.

In order to solve the TL equations using the Method of Characteristics a time domain modal analysis has to be performed. Consider the following pair of 2nx2n matrices:

$$\mathbf{E}_L = \left(\frac{1}{\sqrt{2}}\right)\begin{bmatrix} \mathbf{T}_V^{-1} & \mathbf{Z}_W\mathbf{T}_I^{-1} \\ \mathbf{T}_V^{-1} & -\mathbf{Z}_W\mathbf{T}_I^{-1} \end{bmatrix} \tag{2.17a}$$

$$\mathbf{E}_R = \left(\frac{1}{\sqrt{2}}\right)\begin{bmatrix} \mathbf{T}_V & \mathbf{T}_V \\ \mathbf{T}_I\mathbf{Y}_W & -\mathbf{T}_I\mathbf{Y}_W \end{bmatrix} \tag{2.17b}$$

being $\mathbf{T}_V$ and $\mathbf{T}_I$ the matrices that diagonalize the $\mathbf{L}_{cor}\mathbf{C}$ and $\mathbf{C}\mathbf{L}_{cor}$ products, respectively, and

$$\mathbf{Z}_W = \sqrt{\mathbf{L}_m\mathbf{C}_m^{-1}} \tag{2.18a}$$

$$\mathbf{Y}_W = \sqrt{\mathbf{C}_m\mathbf{L}_m^{-1}} \tag{2.18b}$$

where $\mathbf{L}_m$ and $\mathbf{C}_m$ are the modal inductance and capacitance diagonal matrices defined by

$$\mathbf{L}_m = \mathbf{T}_V^{-1}\mathbf{L}_{cor}\mathbf{T}_I \tag{2.19a}$$

$$\mathbf{C}_m = \mathbf{T}_I^{-1}\mathbf{C}\mathbf{T}_V \tag{2.19b}$$

By definition system (2.15) represents a hyperbolic system if matrix $\mathbf{A}$ has only real eigenvalues and a complete set of linearly independent eigenvectors [18,32]. It can be shown that matrices $\mathbf{E}_L$ and $\mathbf{E}_R$ diagonalize $\mathbf{A}$:

$$\mathbf{E}_L\mathbf{A}\mathbf{E}_R = \begin{bmatrix} \boldsymbol{\Phi} & 0 \\ 0 & -\boldsymbol{\Phi} \end{bmatrix} \tag{2.20}$$

where $\boldsymbol{\Phi}$ is a diagonal matrix whose non-zero elements are the modal propagation velocities given by

$$\phi_j = \frac{1}{\sqrt{L_{mjj} C_{mjj}}} \tag{2.21}$$

where L_{mjj} and C_{mjj} are the jj-th elements of $\mathbf{L}_m$ and $\mathbf{C}_m$ respectively.

To express the line equations in the required form (2.15) is left multiplied by $\mathbf{E}_L$ yielding

$$\left(\frac{\partial \mathbf{v}_m}{\partial t} + \boldsymbol{\Phi}\frac{\partial \mathbf{v}_m}{\partial x}\right) + \mathbf{Z}_W\left(\frac{\partial \mathbf{i}_m}{\partial t} + \boldsymbol{\Phi}\frac{\partial \mathbf{i}_m}{\partial x}\right) - \boldsymbol{\Phi}\left(\frac{\partial}{\partial x}\mathbf{T}_V^{-1}\right)\mathbf{T}_V\mathbf{v}_m - \mathbf{Z}_W\boldsymbol{\Phi}\left(\frac{\partial}{\partial x}\mathbf{T}_I^{-1}\right)\mathbf{T}_I\mathbf{i}_m \tag{2.22a}$$
$$+\boldsymbol{\Phi}\mathbf{R}_m\mathbf{i}_m + \boldsymbol{\Phi}\mathbf{T}_V^{-1}\boldsymbol{\xi} = \mathbf{0}$$

and

$$\left(\frac{\partial \mathbf{v}_m}{\partial t} - \boldsymbol{\Phi}\frac{\partial \mathbf{v}_m}{\partial x}\right) - \mathbf{Z}_W\left(\frac{\partial \mathbf{i}_m}{\partial t} - \boldsymbol{\Phi}\frac{\partial \mathbf{i}_m}{\partial x}\right) - \boldsymbol{\Phi}\left(\frac{\partial}{\partial x}\mathbf{T}_V^{-1}\right)\mathbf{T}_V\mathbf{v}_m - \mathbf{Z}_W\boldsymbol{\Phi}\left(\frac{\partial}{\partial x}\mathbf{T}_I^{-1}\right)\mathbf{T}_I\mathbf{i}_m \tag{2.22b}$$
$$-\boldsymbol{\Phi}\mathbf{R}_m\mathbf{i}_m - \boldsymbol{\Phi}\mathbf{T}_V^{-1}\boldsymbol{\xi} = \mathbf{0}$$

where $\mathbf{v}_m$ and $\mathbf{i}_m$ are modal vectors of voltage and current defined by

$$\mathbf{v}_m = \mathbf{T}_V^{-1}\mathbf{v}(x,t) \tag{2.23a}$$

$$\mathbf{i}_m = \mathbf{T}_I^{-1}\mathbf{i}(x,t) \tag{2.23b}$$

and $\mathbf{R}_m$ is a nondiagonal modal resistance matrix given by

$$\mathbf{R}_m = \mathbf{T}_V^{-1}\mathbf{R}_{dc}\mathbf{T}_I \tag{2.24}$$

In equations (2.22) it has been taken into account that transformation matrices $\mathbf{T}_V$ and $\mathbf{T}_I$ are function of the x variable. In addition it should be stressed that the modal analysis performed in this work is based on the x dependent real matrix $\mathbf{L}_{cor}\mathbf{C}$ and provides real eigenvalues and eigenvectors. In contrast classic frequency domain modal analysis can give rise to complex transformation matrices.

Consider now the curves on the x-t plane defined by the following differential equations:

$$\phi_j = \pm\frac{dx_j}{dt} \qquad j = 1,\ldots\ldots,n \tag{2.25}$$

where the plus sign corresponds to (2.22a) and the minus sign to (2.22b). Solutions to (2.25) are known as *characteristics* and represent a new coordinates system for equations (2.22). When dealing with uniform transmission lines the characteristics are families of straight lines, in the x-t plane, whose slops correspond to the modal velocities. In the case of NU lines (2.25) defines curves with distance dependent positive or negative derivatives.

Along curves (2.25), equations (2.22) become:

$$\frac{d\mathbf{v}_m}{dt} + \mathbf{Z}_W \frac{d\mathbf{i}_m}{dt} - \frac{d\mathbf{X}}{dt}\left(\frac{d}{dx}\mathbf{T}_V^{-1}\right)\mathbf{T}_V\mathbf{v}_m - \mathbf{Z}_W \frac{d\mathbf{X}}{dt}\left(\frac{d}{dx}\mathbf{T}_I^{-1}\right)\mathbf{T}_I\mathbf{i}_m + \frac{d\mathbf{X}}{dt}\mathbf{R}_m\mathbf{i}_m + \frac{d\mathbf{X}}{dt}\mathbf{T}_V^{-1}\boldsymbol{\xi} = \mathbf{0} \tag{2.26a}$$

for characteristic curves with positive derivative and

$$\frac{d\mathbf{v}_m}{dt} - \mathbf{Z}_W \frac{d\mathbf{i}_m}{dt} - \frac{d\mathbf{X}}{dt}\left(\frac{d}{dx}\mathbf{T}_V^{-1}\right)\mathbf{T}_V\mathbf{v}_m + \mathbf{Z}_W \frac{d\mathbf{X}}{dt}\left(\frac{d}{dx}\mathbf{T}_I^{-1}\right)\mathbf{T}_I\mathbf{i}_m + \frac{d\mathbf{X}}{dt}\mathbf{R}_m\mathbf{i}_m + \frac{d\mathbf{X}}{dt}\mathbf{T}_V^{-1}\boldsymbol{\xi} = \mathbf{0} \tag{2.26b}$$

for characteristic curves with negative derivative. Note also that

$$\frac{d\mathbf{X}}{dt} = diag\left(\frac{dx_j}{dt}\right) \qquad j = 1,\ldots\ldots,n \tag{2.27}$$

2.4 RECURSIVE CONVOLUTION

The vector $\boldsymbol{\xi}$ in the last term of (2.26) involves a convolution of the current $\mathbf{i}(x,t)$ with $\mathbf{h}(x,t)$. The latter function can be expressed in the Laplace domain as a rational function expanded into partial fractions. Therefore the convolution term can be solved using a recursive scheme at each distance point x, as follows:

$$\boldsymbol{\xi}(x,t) = \frac{\partial}{\partial t}\boldsymbol{\gamma}(x,t) \tag{2.28a}$$

$$\boldsymbol{\gamma}(x,t) = \int_0^t \mathbf{h}(x,t-\tau)\mathbf{i}(x,\tau)d\tau \tag{2.28b}$$

In the frequency domain, (2.28b) becomes:

$$\boldsymbol{\Gamma}(x,s) = \mathbf{H}(x,s)\mathbf{I}(x,s) \tag{2.29}$$

Using the vector fitting technique [26] $\mathbf{H}(x,s)$ can be expressed at any distance point, $x=d$, as follows:

$$\mathbf{H}(d,s) = \sum_{l=1}^{N} \mathbf{K}_{d,l}\left[s - \mathbf{p}_{d,l}\right]^{-1} \tag{2.30}$$

Using (2.30), (2.29) can be written as:

$$\boldsymbol{\Gamma}(d,s) = \boldsymbol{\Gamma}_{d,1}(s) + \ldots\ldots\ldots\ldots + \boldsymbol{\Gamma}_{d,N}(s) \tag{2.31}$$

where

$$\boldsymbol{\Gamma}_{d,l}(s) = \mathbf{K}_{d,l}\left[s - \mathbf{p}_{d,l}\right]^{-1}\mathbf{I}(d,s) \qquad l = 1,\ldots\ldots\ldots\ldots,N \tag{2.32}$$

Transforming (2.32) back to the time domain:

$$\frac{d}{dt}\boldsymbol{\gamma}_{d,l}(t) - \mathbf{p}_{d,l}\boldsymbol{\gamma}_{d,l}(t) = \mathbf{K}_{d,l}\mathbf{i}(d,t) \quad , \; l = 1,\ldots\ldots\ldots\ldots,N \tag{2.33}$$

Applying finite differences to (2.33) gives:

$$\boldsymbol{\gamma}_{d,l}^{n+1} = \left[1 - \mathbf{p}_{d,l}\Delta t\right]^{-1}\Delta t\left(\frac{1}{\Delta t}\boldsymbol{\gamma}_{d,l}^{n} + \mathbf{K}_{d,l}\mathbf{i}_{d}^{n+1}\right) \qquad l = 1,\ldots\ldots\ldots\ldots,N \tag{2.34}$$

where superscript n correspond to $t=n\Delta t$ and $n+1$ to $t=(n+1)\Delta t$.

The term $\boldsymbol{\gamma}_{d,l}^{n+1}$ represents the l-th convolution at $x=d$ and $t=(n+1)\Delta t$, then the total convolution (2.28b) is:

$$\boldsymbol{\gamma}_{d}^{n+1} = \sum_{l=1}^{N}\left[1 - \mathbf{p}_{d,l}\Delta t\right]^{-1}\Delta t\left(\frac{1}{\Delta t}\boldsymbol{\gamma}_{d,l}^{n} + \mathbf{K}_{d,l}\mathbf{i}_{d}^{n+1}\right) \tag{2.35}$$

Finally (2.28a) can also be approximated using finite differences:

$$\xi(d,t) = \frac{\partial}{\partial t}\boldsymbol{\gamma}(d,t) \cong \frac{1}{\Delta t}\left(\boldsymbol{\gamma}_{d}^{n+1} - \boldsymbol{\gamma}_{d}^{n}\right) \tag{2.36}$$

2.5 NUMERICAL SOLUTION

Equation (2.26) can be approximated using finite differences. Fig. 2.1 shows a graphical interpretation of the characteristic curves of (2.25) that cross through point E at time $t=T+\Delta t$. Each row of (2.26) is valid only over its characteristics to discretize the x-t plane would give rise to a set of non-regular grids, i.e., one grid for each propagating mode. A more practical way to solve this is by defining a regular grid using the largest propagation velocity. By defining $\Delta x=max(\phi)\Delta t$ for the grid and $\Delta x_j=\phi_j\Delta t$ for each mode, the proposed grid satisfies the Courant-Friedrichs-Lewy condition for the whole set of

modes [18,33]. When using a uniform grid the departure points of the characteristics that intersect at any grid's crossing point are unknown and must be determined through an iterative procedure. Since the transmission line is a time invariant element the iterative procedure is performed only once before starting the transient simulation [19]. Afterwards, the values of modal voltages and currents at the required points are obtained by interpolating the known values at grid's crossing points.

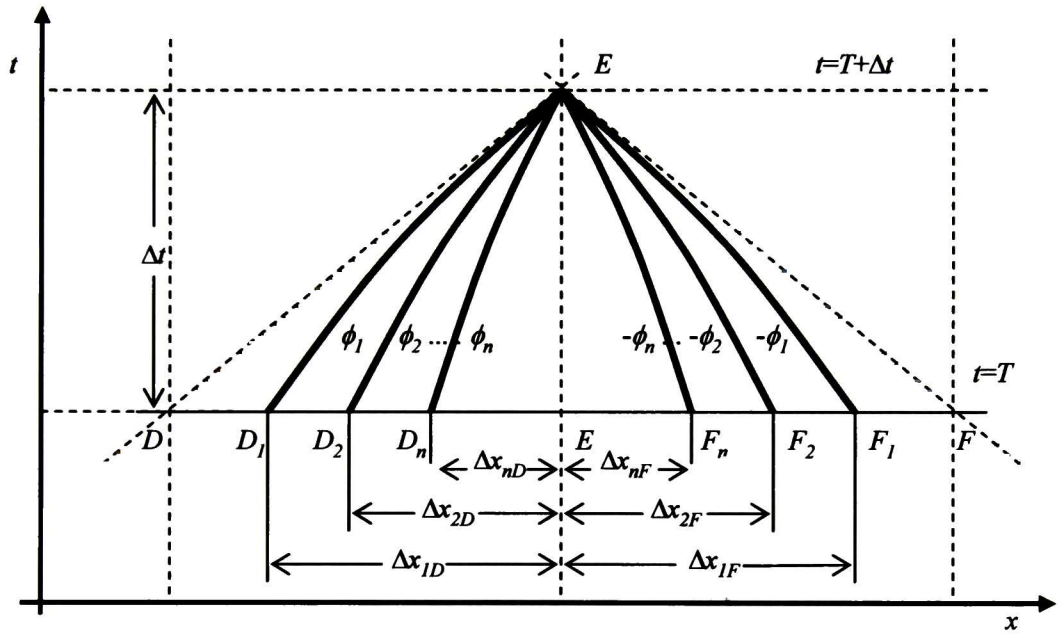

Fig.2.1. Characteristics in the x-t plane

Using finite differences to approximate the derivatives in (2.26) and averages for the required quantities at the evaluation points inside of the line, as shown in Fig.2.1, it can be write

$$\begin{bmatrix} \mathbf{H}_{11} & \mathbf{H}_{12} \\ \mathbf{H}_{21} & -\mathbf{H}_{22} \end{bmatrix} \begin{bmatrix} \mathbf{v}_{mE}^{n+1} \\ \mathbf{i}_{mE}^{n+1} \end{bmatrix} = \begin{bmatrix} \mathbf{f}_{mD}^{n} \\ \mathbf{f}_{mF}^{n} \end{bmatrix} \tag{2.37}$$

where:

$$\mathbf{H}_{11} = \mathbf{U} + \mathbf{T}_{VD}^{-1}\mathbf{T}_{VE} \tag{2.38a}$$

$$\mathbf{H}_{12} = \mathbf{Z}_{WI}(\mathbf{U} + \mathbf{T}_{ID}^{-1}\mathbf{T}_{IE}) + \Delta\mathbf{x}\mathbf{R}_{mI} + (\mathbf{U} + \mathbf{T}_{VE}^{-1}\mathbf{T}_{VE})\Delta\mathbf{x}\mathbf{T}_{VE}^{-1}\boldsymbol{\Psi}_{E}\mathbf{T}_{IE} \tag{2.38b}$$

$$\mathbf{H}_{21} = \mathbf{U} + \mathbf{T}_{VF}^{-1}\mathbf{T}_{VE} \tag{2.38c}$$

$$\mathbf{H}_{22} = \mathbf{Z}_{W2}(\mathbf{U} + \mathbf{T}_{IF}^{-1}\mathbf{T}_{IE}) + \Delta\mathbf{x}\mathbf{R}_{m2} + (\mathbf{U} + \mathbf{T}_{VE}^{-1}\mathbf{T}_{VE})\Delta\mathbf{x}\mathbf{T}_{VE}^{-1}\boldsymbol{\Psi}_E\mathbf{T}_{IE} \tag{2.38d}$$

$$\begin{aligned}\mathbf{f}_{mD}^{n} &= \left[\mathbf{U} + \mathbf{T}_{VE}^{-1}\mathbf{T}_{VD}\right]\mathbf{v}_{mD}^{n} + \left[\mathbf{Z}_{W1}\left(\mathbf{U} + \mathbf{T}_{IE}^{-1}\mathbf{T}_{ID}\right) - \Delta\mathbf{x}\mathbf{R}_{m1}\right]\mathbf{i}_{mD}^{n} \\ &+ \left(\mathbf{U} + \mathbf{T}_{VE}^{-1}\mathbf{T}_{VE}\right)\frac{\Delta\mathbf{x}}{\Delta t}\mathbf{T}_{VE}^{-1}\sum_{l=1}^{N}\boldsymbol{\gamma}_{mEl}^{n} - \left(\mathbf{U} + \mathbf{T}_{VE}^{-1}\mathbf{T}_{VE}\right)\frac{\Delta\mathbf{x}}{\Delta t}\mathbf{T}_{VE}^{-1}\sum_{l=1}^{N}\left[\mathbf{1} + \mathbf{p}_{El}\Delta t\right]^{-1}\boldsymbol{\gamma}_{mEl}^{n}\end{aligned} \tag{2.38e}$$

$$\begin{aligned}\mathbf{f}_{mF}^{n} &= \left[\mathbf{U} + \mathbf{T}_{VE}^{-1}\mathbf{T}_{VF}\right]\mathbf{v}_{mF}^{n} - \left[\mathbf{Z}_{W2}\left(\mathbf{U} + \mathbf{T}_{IE}^{-1}\mathbf{T}_{IF}\right) - \Delta\mathbf{x}\mathbf{R}_{m2}\right]\mathbf{i}_{mF}^{n} \\ &- \left(\mathbf{U} + \mathbf{T}_{VE}^{-1}\mathbf{T}_{VE}\right)\frac{\Delta\mathbf{x}}{\Delta t}\mathbf{T}_{VE}^{-1}\sum_{l=1}^{N}\boldsymbol{\gamma}_{mEl}^{n} + \left(\mathbf{U} + \mathbf{T}_{VE}^{-1}\mathbf{T}_{VE}\right)\frac{\Delta\mathbf{x}}{\Delta t}\mathbf{T}_{VE}^{-1}\sum_{l=1}^{N}\left[\mathbf{1} + \mathbf{p}_{El}\Delta t\right]^{-1}\boldsymbol{\gamma}_{mEl}^{n}\end{aligned} \tag{2.38f}$$

being **U** the identity matrix and

$$\Delta\mathbf{x} = diag(\Delta x_1, \Delta x_2, ..., \Delta x_n) \tag{2.39a}$$

$$\mathbf{Z}_{W1} = (\mathbf{Z}_{WE} + \mathbf{Z}_{WD})/2 \qquad \mathbf{Z}_{W2} = (\mathbf{Z}_{WE} + \mathbf{Z}_{WF})/2 \tag{2.39b}$$

$$\mathbf{R}_{m1} = (\mathbf{R}_{mE} + \mathbf{R}_{mD})/2 \qquad \mathbf{R}_{m2} = (\mathbf{R}_{mE} + \mathbf{R}_{mF})/2 \tag{2.39c}$$

$$\boldsymbol{\Psi}_E = \sum_{l=1}^{N}\mathbf{K}_{El}\left[\mathbf{1} + \mathbf{p}_{El}\Delta t\right]^{-1} \tag{2.39d}$$

the subscript "*n*" indicates any time step and "*n+1*" indicates the next time step. The letters *D*, *E* and *F* in the subscripts indicate the position at which quantities are calculated, as shown in Fig.2.1. By solving (2.37) voltages and currents at point E at time $t=T+\Delta t$ can be found when modal voltages and currents at time $t=T$ are known.

2.6 ITERATIVE PROCEDURE

When using a uniform grid the departure points of the characteristics that intersect at any crossing point of the grid are unknown and must be determined through an iterative procedure [34]. Since the TL is a time invariant element the iterative procedure is performed only once, before starting the transient simulation. Afterwards, the values of modal voltages and currents at the required points are obtained by interpolating the known values at the crossing points of the grid.

To find the crossing points of the characteristics with the horizontal line at t=T the following procedure is applied:

1. – For each propagation velocity ϕ_{jE} calculate the distance Δx_{jD} (distance from E to Dj) and distance Δx_{jF} (distance from point Fj to point E):

$$\Delta x_{jD} = \phi_{jE} \Delta t \qquad \Delta x_{jF} = \Delta x_{jD} \tag{2.40a,b}$$

2. With the position of the cross points calculate propagation velocities at points Dj and Fj:

$$\mathbf{\Phi}_D = \sqrt{\mathbf{L}_D'^{-1}\mathbf{C}_D'^{-1}} \qquad \mathbf{\Phi}_F = \sqrt{\mathbf{L}_F'^{-1}\mathbf{C}_F'^{-1}} \tag{2.41a,b}$$

3. – To make a new estimation of the velocities, calculate an average between the calculated velocities at D and F with that of point E:

$$\mathbf{\Phi}_D = (\mathbf{\Phi}_E + \mathbf{\Phi}_D)/2 \qquad \mathbf{\Phi}_F = (\mathbf{\Phi}_E + \mathbf{\Phi}_F)/2 \tag{2.42a,b}$$

4. - Calculate again distances Δx_{jD} and Δx_{jF} :

$$\Delta x_{jD} = \phi_{jD} \Delta t \qquad \Delta x_{jF} = \phi_{jF} \Delta t \tag{2.43a,b}$$

5.- Repeat points 2, 3 and 4 until the difference between the current and past values of the distances Δx_{jD} and Δx_{jF} are lower that some established tolerance.

2.7 BOUNDARY CONDITIONS

At the sending end of the line there exist only n characteristic curves, which correspond to the bottom sign of equation (2.26), as shown in Fig.2.2. Using the second row of equation (2.37):

$$\mathbf{H}_{21}\mathbf{v}_{mE}^{n+1} - \mathbf{H}_{22}\mathbf{i}_{mE}^{n+1} = \mathbf{f}_{mF}^{n} \tag{2.44}$$

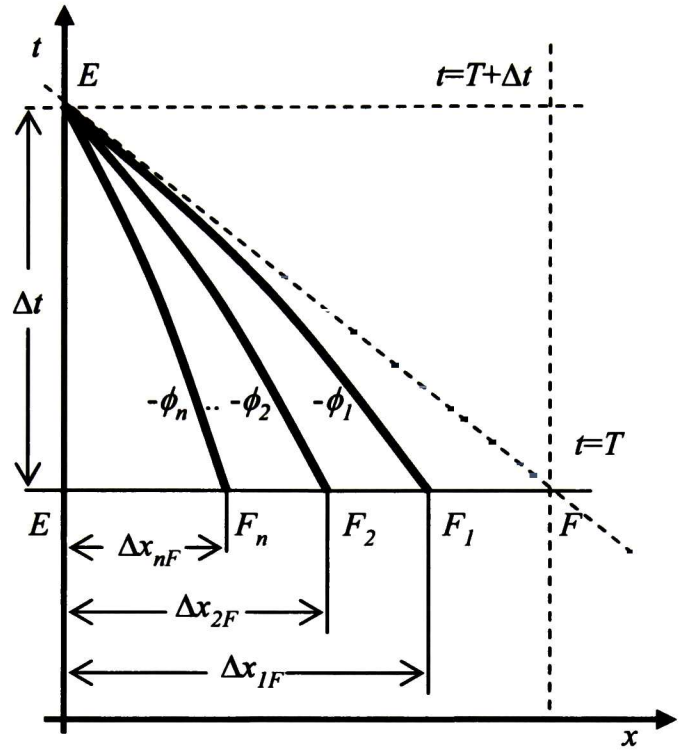

Fig.2.2. Characteristics curves at the sending end of the transmission line.

Using the modal transformations, (2.44) can be rearranged in the conductors domain as:

$$\mathbf{i}_e^{n+1} = \mathbf{Y}_e \mathbf{v}_e^{n+1} - \mathbf{i}_{histe} \tag{2.45}$$

where

$$\mathbf{Y}_e = \mathbf{T}_{IE}\mathbf{H}_{22}^{-1}\mathbf{H}_{21}^{-1}\mathbf{T}_{VE}^{-1} \tag{2.46a}$$

$$\mathbf{i}_{histe} = \mathbf{T}_{IE}\mathbf{H}_{22}^{-1}\mathbf{f}_{mF}^{n} \tag{2.46b}$$

$$\mathbf{v}_e^{n+1} = \mathbf{T}_{VE}\mathbf{v}_{mE}^{n+1} \tag{2.46c}$$

$$\mathbf{i}_e^{n+1} = \mathbf{T}_{IE}\mathbf{i}_{mE}^{n+1} \tag{2.46d}$$

In the same manner at the receiving end there exist only the n characteristics with positive derivatives as shown in Fig.2.3. From the first row of (2.37):

$$\mathbf{H}_{11}\mathbf{v}_{mE}^{n+1} + \mathbf{H}_{12}\mathbf{i}_{mE}^{n+1} = \mathbf{f}_{mD}^{n} \tag{2.47}$$

Using again the modal transformations (2.47) gives in the conductors domain:

$$\mathbf{i}_r^{n+1} = \mathbf{Y}_r \mathbf{v}_r^{n+1} - \mathbf{i}_{histr} \tag{2.48}$$

where

$$\mathbf{Y}_r = \mathbf{T}_{IE}\mathbf{H}_{12}^{-1}\mathbf{H}_{11}^{-1}\mathbf{T}_{VE}^{-1} \tag{2.49a}$$

$$\mathbf{i}_{histr} = \mathbf{T}_{IE}\mathbf{H}_{12}^{-1}\mathbf{f}_{mD}^{n} \tag{2.49b}$$

$$\mathbf{v}_r^{n+1} = \mathbf{T}_{VE}\mathbf{v}_{mE}^{n+1} \tag{2.49c}$$

$$\mathbf{i}_r^{n+1} = -\mathbf{T}_{IE}\mathbf{i}_{mE}^{n+1} \tag{2.49d}$$

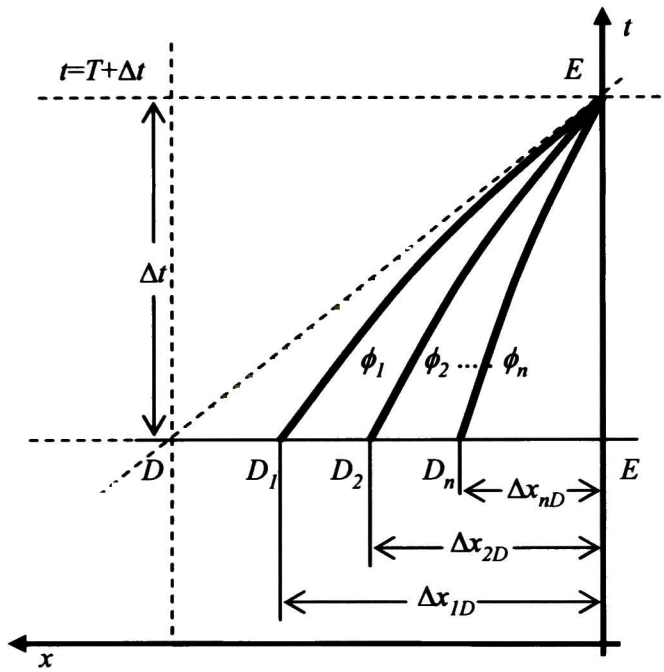

Fig.2.3. Characteristics curves at the receiving end of the transmission line

Equations (2.45) and (2.48) represent a Norton model for the transmission line ends, as shown in Fig.2.4. Current sources $\mathbf{i}_{histe}$ and $\mathbf{i}_{histr}$ at any time t are given in terms of modal voltages and currents calculated at time t-Δt at the first and last interior points. Therefore at time t the transmission line ends are topologically disconnected.

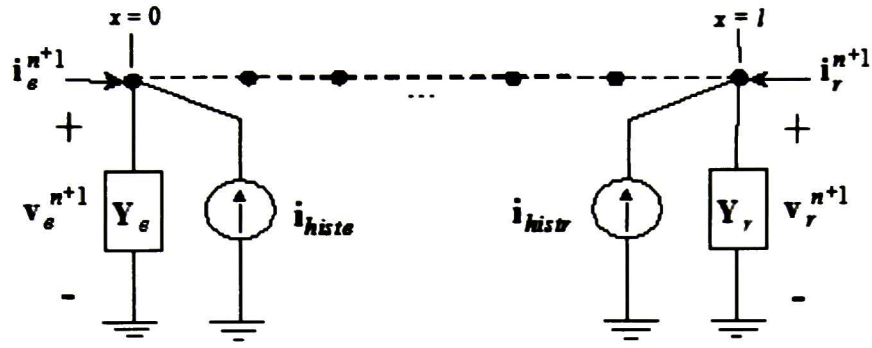

Fig.2.4. Norton equivalent circuit for the transmission line's ends.

2.8 APPLICATION EXAMPLE

As an example consider a highly NU three-phase TL crossing a hilly terrain, as shown in Fig.2.5. The line is formed by parallel conductors with 2.54 cm. radius and 10 m. of horizontal separation; the ground resistivity is assumed to be 100 Ω-m. A unit step voltage was applied to the conductors at the sending end and the receiving end was left open. Source resistances of 10 Ω were used.

The number of time steps for the simulation with the NLTP was 512 and for the EMTP, Method of Characteristics and Piecewise Uniform Form were 400. The number of line segments in cascade connection for the three programs was 20. In order to take into account the frequency dependence of the electrical parameters of each line in the EMTP, the J. Marti model was used. Figures 2.6, 2.7 and 2.8 shown the voltage at phase C of the receiving node obtained with the Method of Characteristics, Piecewise Uniform Form and EMTP, respectively, compared against Numerical Laplace Transform results.

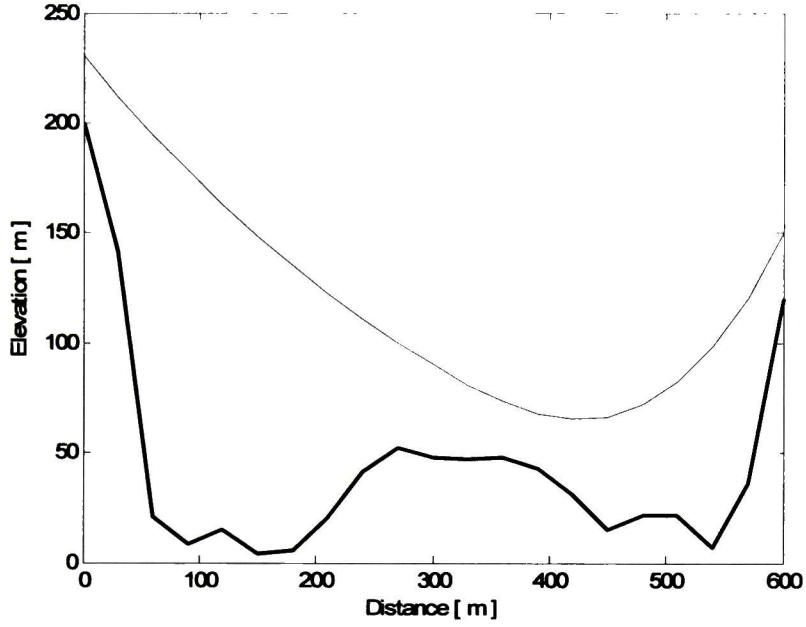

Fig.2.5. Nonuniform Transmission Line geometry.

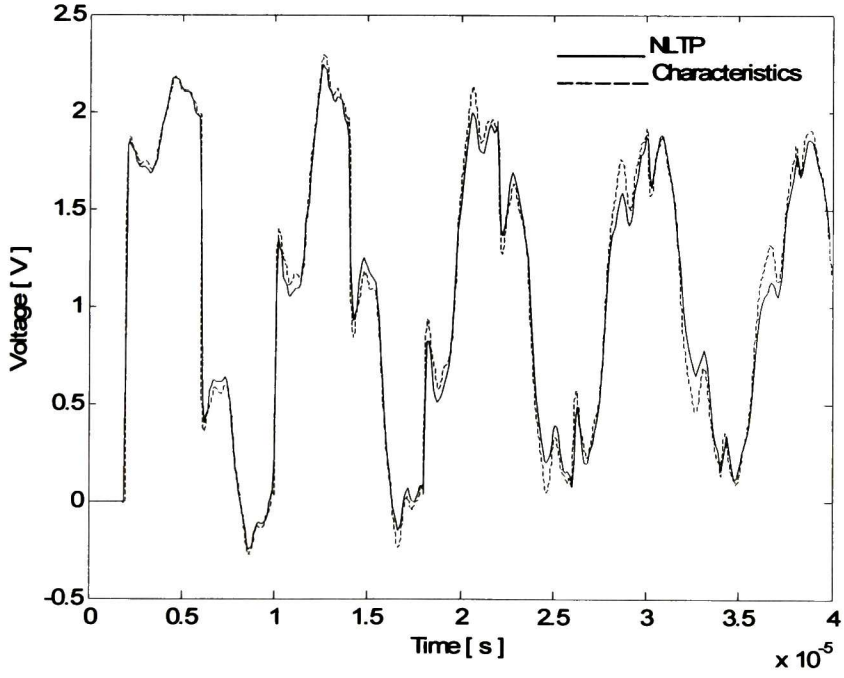

Fig.2.6. Waveform at the phase C of the receiving node of a nonuniform three-phase line: NLTP and Method of Characteristics.

Fig. 2.7 shows waveforms obtained by considering a frequency dependent equivalent uniform TL with a height of 26.59 m. This value was obtained using the average distance between the conductors and the terrain. Results from Figs. 2.6 and 2.7 show a remarkable difference in the transient waveform when non uniformities are considered

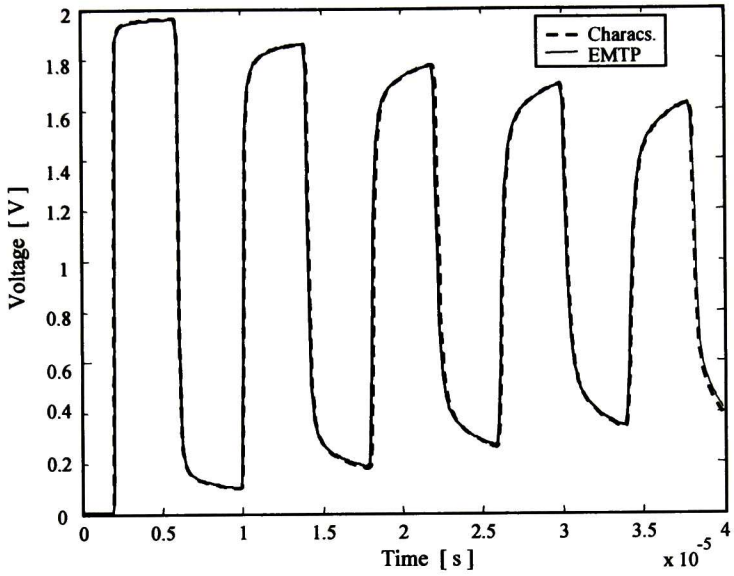

Fig.2.7. Waveform at the phase C of the receiving node of a uniform three-phase line: EMTP and Method of Characteristics.

As can be seen from Figs. 2.6 and 2.7 the three methods, i.e., Characteristics, EMTP and NLTP, yield almost the same results. It should be noticed the practical difficulty involved when using the EMTP or NLTP. With both methods the transmission line has to be divided in several segments and each one must be included as a uniform transmission line by itself. For a particular simulation the user has to decide about the number of segments based on his expertise. When a new simulation with a different number of segments is required, the electrical parameters have to be calculated again and a new data file (or network) has to be created. This procedure in practice can be very cumbersome and lengthy for the user.

A comparison between computing a different set of poles and residues for each line segment and using the same set of poles, with different residues, for the whole line was made applying the Method of Characteristics. Sets of poles computed at a number of heights between the minimum and maximum line heights were tried. The maximum

relative error, with respect to the maximum voltage, was 2%. In some cases using a single set of poles was faster than using different sets, but in other cases the contrary occurred. For both outcomes the maximum absolute difference in computation time was about 8%. Figure 2.8 shows waveforms using different sets of poles and the same set of poles calculated at the average height.

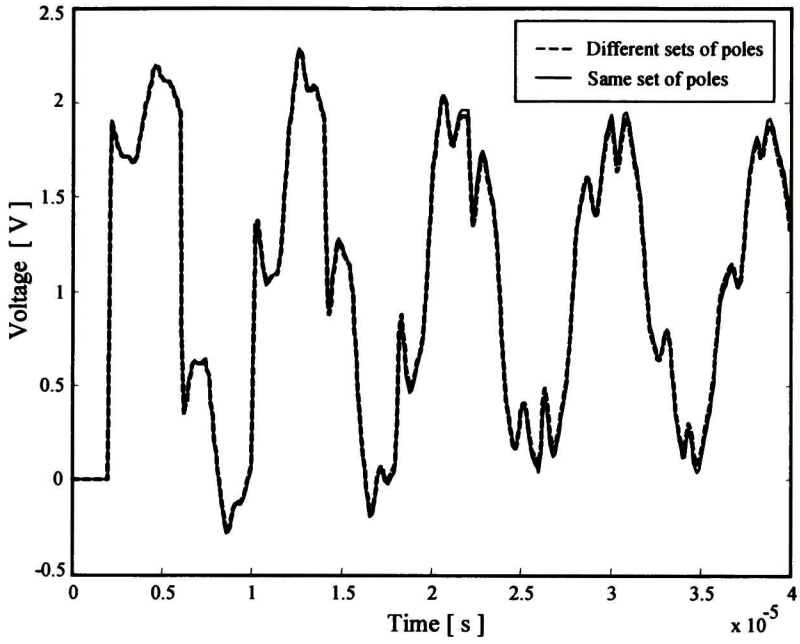

Fig. 2.8. Waveforms using a different set of poles for each line segment and using the same set of poles for all the line segments.

2.9 OBSERVATIONS

The Method of Characteristics has been applied to the analysis of electromagnetic transients in Nonuniform Multiconductor TLs with frequency dependent electrical parameters. To solve the TL equations, a time domain modal analysis that yields real eigenvalues and eigenvectors has been performed. To include the frequency dependence of the electrical parameters the convolution operation has been simplified by using the vector fitting technique. In addition Norton models for the transmission line ends have been developed in order to make the method suitable to be included into general purpose programs. The proposed model can be applied for any geometrical configuration and does

not require damping techniques. Therefore it could help to determine whether the oscillations, or the lack of them, presented in time domain analysis are part of the transient phenomenon or due to numerical errors.

3 PIECEWISE UNIFORM MODEL FOR NONUNIFORM MULTICONDUCTOR TRANSMISSION LINES

3.1 INTRODUCTION

In the method of characteristics for Nonuniform multiconductor TLs computing spatial derivatives of the modal transformation matrices is required. In addition, since the characteristics curves posses distance dependent slops, launching points for the characteristics have to be approximated by an iterative procedure.

In this chapter a new model for NU multiconductor TLs with frequency dependent parameters using the method of characteristics is presented. This model considers the transmission line as being formed by a series of small Uniform Transmission Lines. With this approach spatial derivatives of modal transformation matrices are not required and launching points for the characteristics are always known. Non uniformities of overhead TLs can result from changes of conductor's height or radius, or variations of the electrical properties of conductors and terrain. In particular in this chapter non uniformities due to sagging of conductors are considered again as an example. Results obtained with the proposed model are compared with those from a Numerical Laplace Transform Program (NLTP)

3.2 PIECEWISE MODEL

Along the characteristics the transmission line equations become:

$$\frac{d\mathbf{v}_m}{dt}+\mathbf{Z}_w\frac{d\mathbf{i}_m}{dt}-\frac{d\mathbf{X}}{dt}\left(\frac{d}{dx}\mathbf{T}_V^{-1}\right)\mathbf{T}_V\mathbf{v}_m-\mathbf{Z}_w\frac{d\mathbf{X}}{dt}\left(\frac{d}{dx}\mathbf{T}_I^{-1}\right)\mathbf{T}_I\mathbf{i}_m+\frac{d\mathbf{X}}{dt}\mathbf{R}_m\mathbf{i}_m+\frac{d\mathbf{X}}{dt}\mathbf{T}_V^{-1}\boldsymbol{\xi}=\mathbf{0} \quad (3.1a)$$

$$\frac{d\mathbf{v}_m}{dt}-\mathbf{Z}_w\frac{d\mathbf{i}_m}{dt}-\frac{d\mathbf{X}}{dt}\left(\frac{d}{dx}\mathbf{T}_V^{-1}\right)\mathbf{T}_V\mathbf{v}_m+\mathbf{Z}_w\frac{d\mathbf{X}}{dt}\left(\frac{d}{dx}\mathbf{T}_I^{-1}\right)\mathbf{T}_I\mathbf{i}_m+\frac{d\mathbf{X}}{dt}\mathbf{R}_m\mathbf{i}_m+\frac{d\mathbf{X}}{dt}\mathbf{T}_V^{-1}\boldsymbol{\xi}=\mathbf{0} \quad (3.1b)$$

where

$$\frac{d\mathbf{X}}{dt} = \text{diag}\left(\frac{dx_j}{dt}\right), \; j = 1,\ldots,q \tag{3.2}$$

The vector $\boldsymbol{\xi}$ in the last term of (3.1) involves a convolution of the current $\mathbf{i}(x,t)$ with $\mathbf{h}(x,t)$. The latter function can be expressed in the Laplace domain as a rational function expanded into partial fractions. Therefore the convolution term can be solved using a recursive scheme at each distance point x, as presented in detail in chapter 2.

Equations (3.1) can be approximated using finite differences over the characteristic curves. Since the characteristics are curves with distance dependent slops the departure points of the characteristics that intersect at any crossing point of the grid are unknown and must be determined through an iterative procedure [14]. In this chapter a more practical method is presented. It consists on considering the transmission line as a cascade connection of small uniform transmission lines. This allows knowing the departure points and does not require calculation of the space derivatives of the transformation matrices. Hence (3.1a) and (3.1b) become:

$$\frac{d\mathbf{v}_m}{dt} + \mathbf{Z}_w \frac{d\mathbf{i}_m}{dt} + \frac{d\mathbf{X}}{dt}\mathbf{R}_m\mathbf{i}_m + \frac{d\mathbf{X}}{dt}\mathbf{T}_V^{-1}\boldsymbol{\xi} = \mathbf{0} \tag{3.3a}$$

and

$$\frac{d\mathbf{v}_m}{dt} - \mathbf{Z}_w \frac{d\mathbf{i}_m}{dt} + \frac{d\mathbf{X}}{dt}\mathbf{R}_m\mathbf{i}_m + \frac{d\mathbf{X}}{dt}\mathbf{T}_V^{-1}\boldsymbol{\xi} = \mathbf{0} \tag{3.3b}$$

By defining $\Delta x = max(\phi_j)\Delta t$ for the grid and $\Delta x_j = \phi_j \Delta t$ for each mode, as shown in Fig. 3.1, the grid will satisfy the Courant-Friedrichs-Lewy condition for the whole set of modes [28]. Note that the transmission line sections at both sides of point E do not have the same electrical parameters, therefore the slop of the characteristics on the right side do not have the same absolute value of the corresponding slops on the left side.

Using finite differences over the straight lines shown in Fig. 3.1 to approximate the derivatives in (3.3) and averages for the required quantities at the evaluation points, it can be written:

$$\frac{\mathbf{v}_{mE} - \mathbf{v}_{mD}}{\Delta t} + \mathbf{Z}_{wD}\frac{\mathbf{i}_{mE} - \mathbf{i}_{mD}}{\Delta t} + \frac{\Delta\mathbf{X}}{\Delta t}\frac{\mathbf{R}_{mD}(\mathbf{i}_{mE} + \mathbf{i}_{mD})}{2} + \frac{\Delta\mathbf{X}}{\Delta t}\frac{\mathbf{T}_{VD}^{-1}(\boldsymbol{\xi}_E + \boldsymbol{\xi}_D)}{2} = \mathbf{0} \tag{3.4}$$

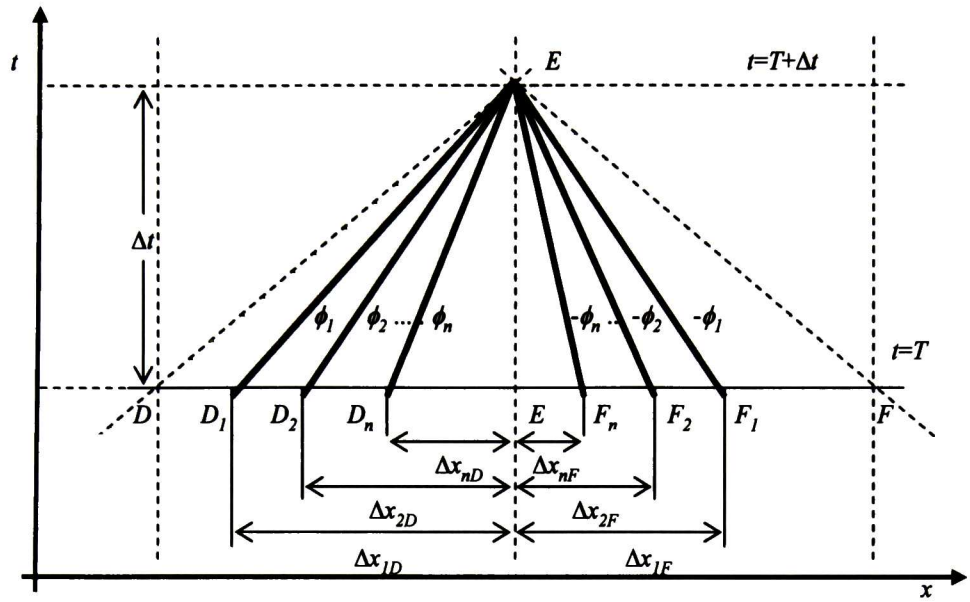

Fig. 3.1. Characteristics in the *x-t* plane.

and

$$\frac{\mathbf{v}_{mF}-\mathbf{v}_{mE}}{\Delta t}-\mathbf{Z}_{wF}\frac{\mathbf{i}_{mF}-\mathbf{i}_{mE}}{\Delta t}+\frac{\Delta \mathbf{X}}{\Delta t}\frac{\mathbf{R}_{mF}(\mathbf{i}_{mF}+\mathbf{i}_{mE})}{2}+\frac{\Delta \mathbf{X}}{\Delta t}\frac{\mathbf{T}_{VF}^{-1}(\boldsymbol{\xi}_F+\boldsymbol{\xi}_E)}{2}=\mathbf{0} \tag{3.5}$$

Rearranging and grouping terms the following linear system is obtained:

$$\begin{bmatrix}\mathbf{Y}_r & \mathbf{U}\\ \mathbf{Y}_e & -\mathbf{U}\end{bmatrix}\begin{bmatrix}\mathbf{v}_e^{n+1}\\ \mathbf{i}_e^{n+1}\end{bmatrix}=\begin{bmatrix}\mathbf{i}_{histr}\\ \mathbf{i}_{histe}\end{bmatrix} \tag{3.6}$$

where:

$$\mathbf{Y}_r=\mathbf{T}_{ID}\left(\mathbf{Z}_{WD}+(\Delta\mathbf{x}/2)\mathbf{R}_{mD}+\Delta\mathbf{x}\mathbf{T}_{VD}^{-1}\boldsymbol{\Psi}_D\mathbf{T}_{ID}\right)^{-1}\mathbf{T}_{VE}^{-1} \tag{3.7a}$$

$$\mathbf{i}_{histr}=\mathbf{T}_{ID}\left(\mathbf{Z}_{WD}+(\Delta\mathbf{x}/2)\mathbf{R}_{mD}+\Delta\mathbf{x}\mathbf{T}_{VD}^{-1}\boldsymbol{\Psi}_D\mathbf{T}_{ID}\right)^{-1}\mathbf{T}_{VD}^{-1}\mathbf{v}_{histD} \tag{3.7b}$$

$$\mathbf{Y}_e=\mathbf{T}_{IF}\left(\mathbf{Z}_{WF}+(\Delta\mathbf{x}/2)\mathbf{R}_{mF}+\Delta\mathbf{x}\mathbf{T}_{VF}^{-1}\boldsymbol{\Psi}_F\mathbf{T}_{IF}\right)^{-1}\mathbf{T}_{VF}^{-1} \tag{3.7c}$$

$$\mathbf{i}_{histe}=\mathbf{T}_{IF}\left(\mathbf{Z}_{WF}+(\Delta\mathbf{x}/2)\mathbf{R}_{mF}+\Delta\mathbf{x}\mathbf{T}_{VF}^{-1}\boldsymbol{\Psi}_F\mathbf{T}_{IF}\right)^{-1}\mathbf{T}_{VF}^{-1}\mathbf{v}_{histF} \tag{3.7d}$$

$$\begin{aligned}\mathbf{v}_{histD}=\mathbf{T}_{VD}\{\,&\mathbf{v}_{mD}^n-\left[\mathbf{Z}_{WD}+(\Delta\mathbf{x}/2)\mathbf{R}_{mD}\right]\mathbf{i}_{mD}^n\\&-\frac{\Delta\mathbf{x}}{\Delta t}\mathbf{T}_{VD}^{-1}\sum_{l=1}^{N}\boldsymbol{\gamma}_{mDl}^n+\frac{\Delta\mathbf{x}}{\Delta t}\mathbf{T}_{VD}^{-1}\sum_{l=1}^{N}\left[1+\mathbf{p}_{Dl}\Delta t\right]^{-1}\boldsymbol{\gamma}_{mDl}^n\}\end{aligned} \tag{3.7e}$$

$$\mathbf{v}_{histF} = \mathbf{T}_{VF}\{\mathbf{v}'_{mF} + [\mathbf{Z}_{WF} - (\Delta\mathbf{x}/2)\mathbf{R}_{mF}]\,\mathbf{i}^{n}_{mF} + \frac{\Delta\mathbf{x}}{\Delta t}\mathbf{T}^{-1}_{VF}\sum_{l=1}^{N}\boldsymbol{\gamma}^{n}_{mFl} - \frac{\Delta\mathbf{x}}{\Delta t}\mathbf{T}^{-1}_{VF}\sum_{l=1}^{N}[1+\mathbf{p}_{Fl}\Delta t]^{-1}\boldsymbol{\gamma}'_{mFl}\} \tag{3.7f}$$

where

$$\Delta\mathbf{x} = diag(\Delta x_1, \Delta x_2, ..., \Delta x_n) \tag{3.8a}$$

$$\boldsymbol{\Psi}_{D,F} = \sum_{l=1}^{N}\mathbf{K}_{D,Fl}(1+\mathbf{p}_{D,Fl}\Delta t)^{-1} \tag{3.8b}$$

$$\mathbf{U} = \text{identity matrix} \tag{3.8c}$$

The subscript "n" indicates any time step and "$n+1$" indicates the next time step. The letters D, E and F in the subscripts indicate the points where quantities are calculated, as shown in Fig. 3.1. By solving (3.6) voltages and currents at point E at time $t=T+\Delta t$ can be found when voltages and currents at time $t=T$ are known.

3.3 BOUNDARY CONDITIONS

At the sending end of the line there exist only q characteristic curves, which correspond to (3.5). Using the second row of equation (3.6):

$$\mathbf{i}^{n+1}_{1} = \mathbf{Y}_{e}\mathbf{v}^{n+1}_{1} - \mathbf{i}_{histe} \tag{3.9}$$

where subscript "1" has been used instead of subscript "e" to indicate the initial point of the transmission line.

In a similar manner at the receiving end there exist only the characteristics that correspond to (3.4). From the first row of (3.6) it can be written

$$\mathbf{i}^{n+1}_{2} = \mathbf{Y}_{r}\mathbf{v}^{n+1}_{2} - \mathbf{i}_{histr} \tag{3.10}$$

where instead of subscript "e" subscript "2" has been used to indicate the final point of the transmission line and

$$\mathbf{i}^{n+1}_{2} = -\mathbf{i}^{n+1}_{e} \tag{3.11}$$

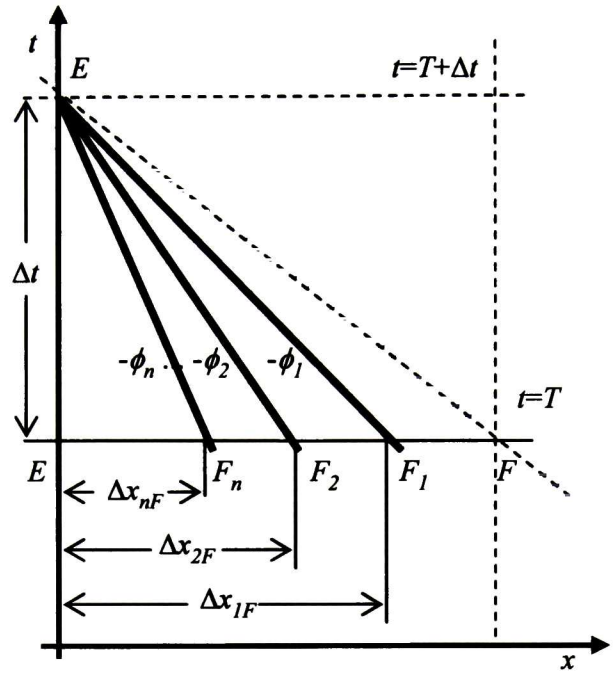

Fig.3.2. Characteristic at the sending end of the line

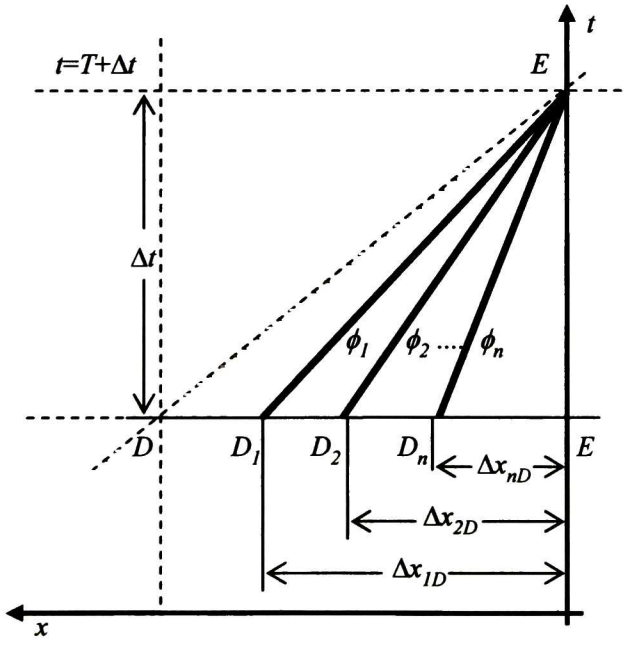

Fig.3.3. Characteristics at the receiving end of the line.

Equations (3.9) and (3.10) represent Norton models for the transmission line ends. Current sources i_{histe} and i_{histr} at any time step t are given in terms of modal voltages and currents calculated at time t-Δt at the first and last interior points, respectively. Therefore at time t the transmission line ends are topologically disconnected.

3.4 APPLICATION EXAMPLES

a) As an example consider a highly NU three-phase TL crossing a hilly terrain, as shown in Fig.3.4. The line is formed by parallel conductors with 2.54 cm. radius and 10 m. horizontal separation; the ground resistivity is assumed to be 100 Ω-m. A unit step voltages was applied to the conductors at the sending end and the receiving end was left open. Source resistances of 10 Ω were used.

The number of time steps for the simulation with the NLTP was 512 and for the EMTP, Method of Characteristics and Piecewise Uniform Form were 400. The number of line segments in cascade connection for the three programs was 20. In order to take into account the frequency dependence of the electrical parameters of each line in the EMTP, the J. Marti model was used. Fig. 3.5, 3.6 and 3.7 shown the voltage at phase C of the receiving node obtained with the Method of Characteristics, Piecewise Uniform Form and EMTP, respectively, compared against Numerical Laplace Transform results.

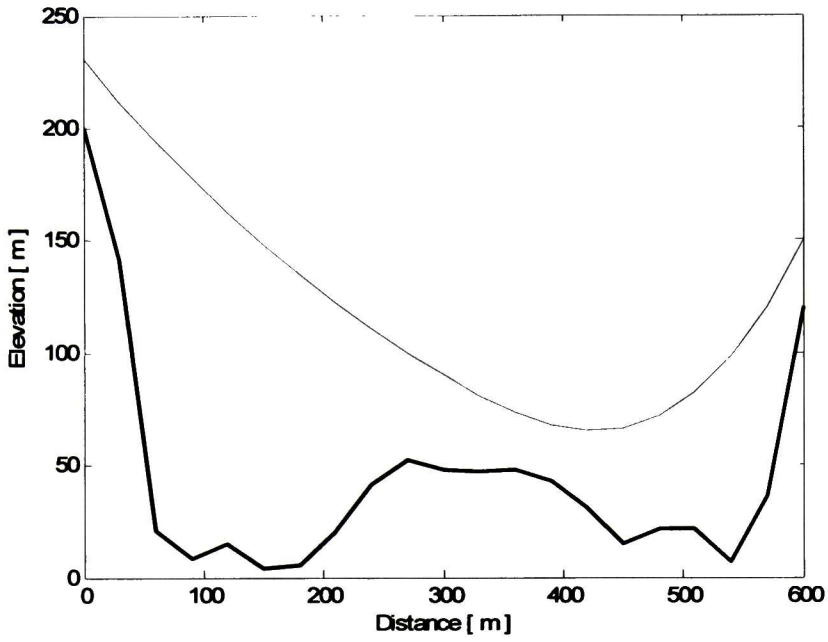

Fig.3.4. Nonuniform Transmission Line geometry.

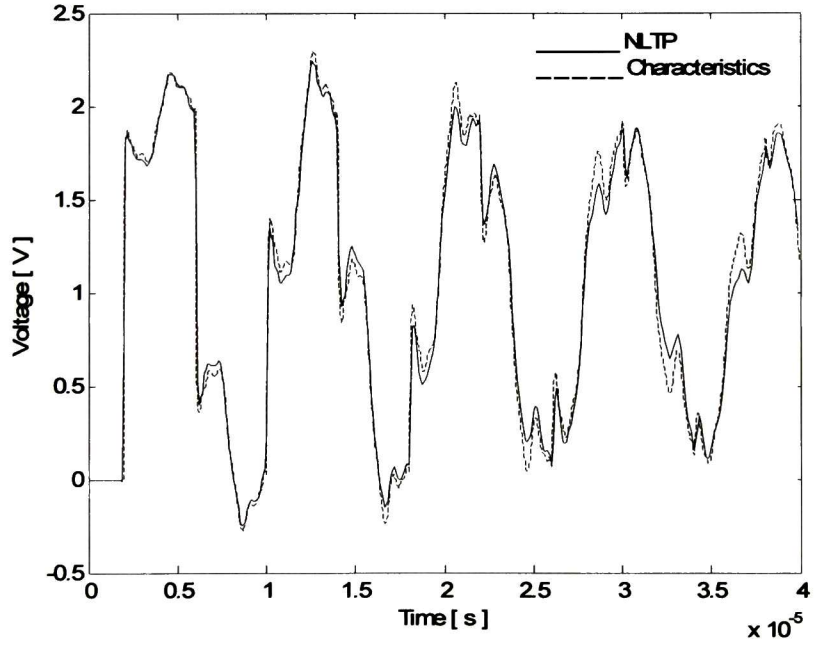

Fig.3.5. Waveform at the phase C of the receiving node of a nonuniform three-phase line: NLTP and Method of Characteristics.

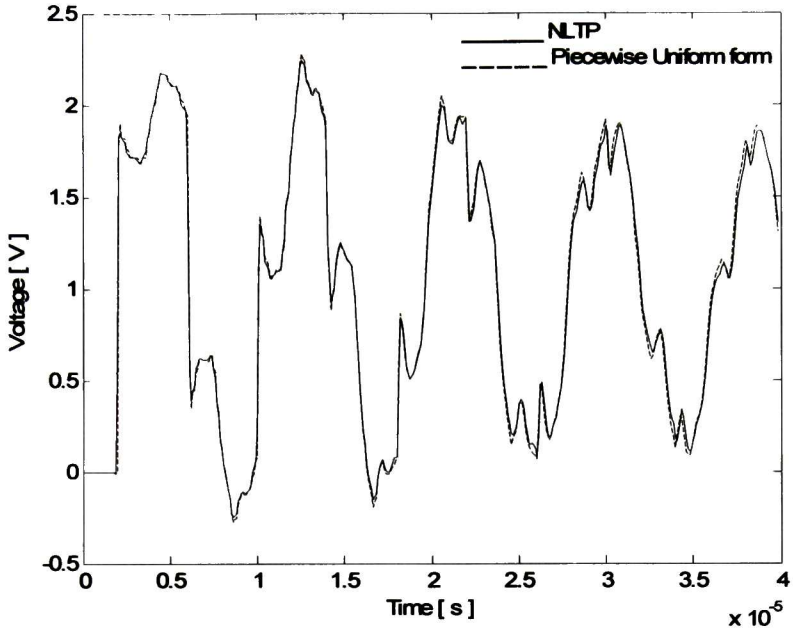

Fig.3.6. Waveform at the phase C of the receiving node of a nonuniform three-phase line: NLTP and Piecewise Uniform form.

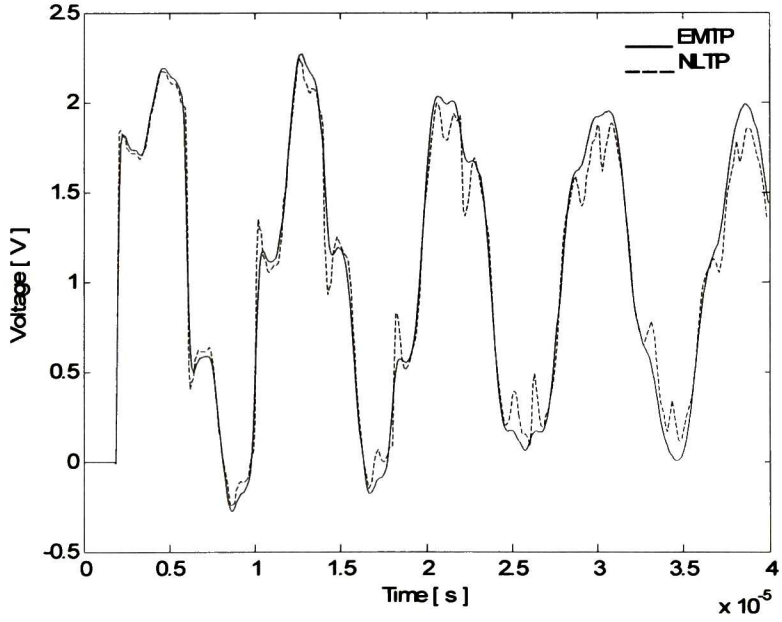

Fig.3.7. Waveform at the phase C of the receiving node of a nonuniform three-phase line: EMTP and NLTP

b) As a second example consider a Vertical Multiconductor system as is shown at Fig.3.8. The system is formed by four vertical conductors with 0.05 m. radius and 1 m. horizontal separation; the ground resistivity is assumed to be 30 Ω-m. A current source as is shown in Fig.3.9 was applied with a sources resistance of 250Ω. The number of line segments in cascade connection was 30 for each simulation program. Fig.3.10 shown the voltage at the top node obtained with the Method of Characteristics (Piecewise Uniform Form) compared against Numerical Laplace Transform results.

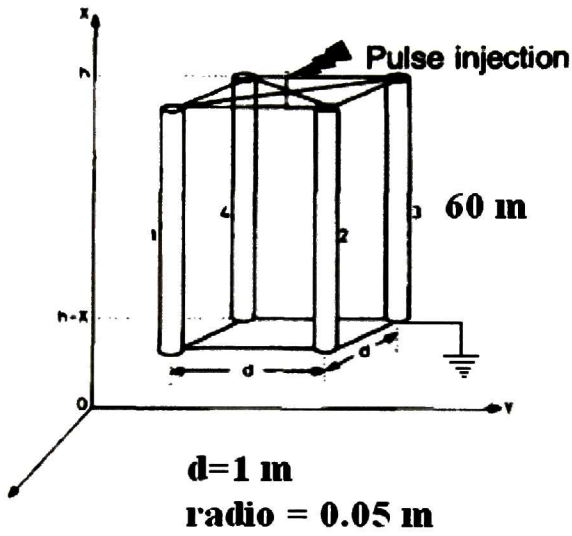

Fig.3.8. Vertical Multiconductor Transmission Line System.

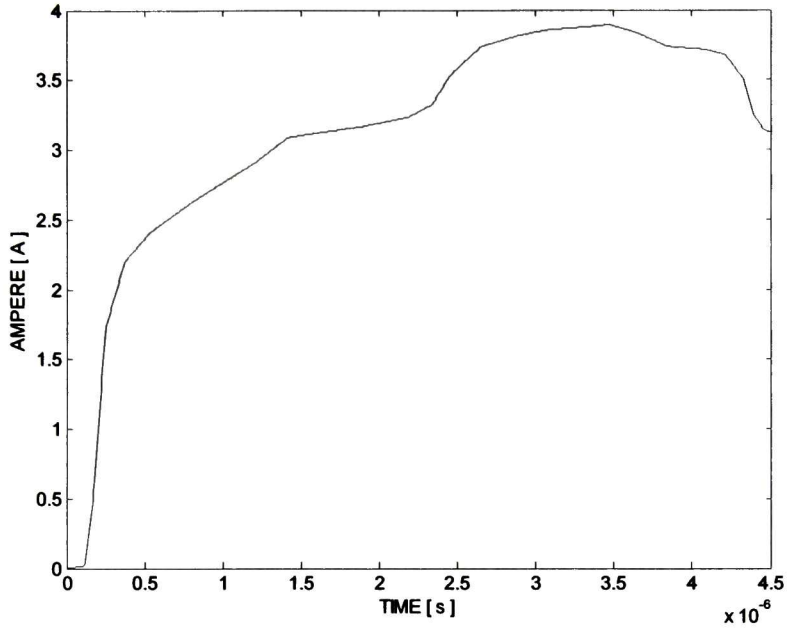

Fig.3.9. Current Source injected at the top of the vertical transmission lines system.

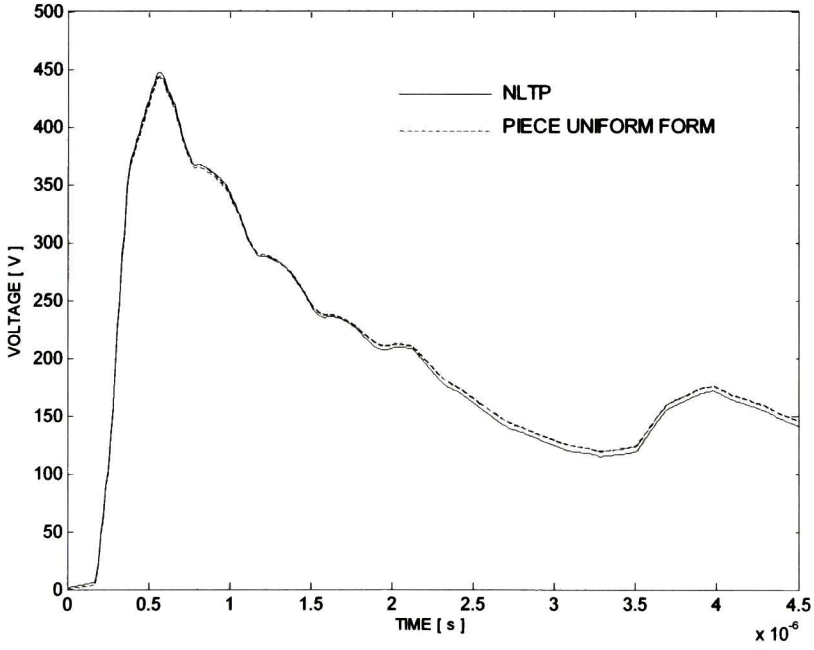

Fig.3.10. Voltages at the top of the Vertical Multiconductor Transmission Line System.

3.5 OBSERVATIONS

In this Chapter the Method of Characteristics has been applied to the analysis of electromagnetic transients in NU multiconductor TLs with frequency dependent electrical parameters. The Nonuniform transmission line has been modeled as a piece-wise uniform line, this is, as a cascade connection of small uniform transmission lines. This model does not require the spatial derivatives of the transformation matrices, therefore yields computing time savings. The proposed model provides good results and can be applied to any geometrical configuration.

4 FINITE DIFFERENCE TIME DOMAIN METHOD FOR FIELD EXCITED NONUNIFORM MULTICONDUCTOR TRANSMISSION LINES

4.1 INTRODUCTION

One of most widely applied numerical method for the computation of electromagnetic fields is the Finite Differences Time Domain method (FDTD) or Yee's Method [35]. Since this method is very fast and is not difficult to understand, in this chapter is applied to solve the Nonuniform transmission line equations taking into account external electromagnetic fields and frequency dependent parameters.

4.2 NONUNIFORM MULTICONDUCTOR TRANSMISSION LINE EQUATIONS WITH INCIDENT ELECTROMAGNETIC FIELDS

From the Charge Conservation equation one can derive a modified version of the Telegraphers' equations proposed by Radulet, et al [24] for Transmission Lines taking into account frequency dependent parameters and external Electromagnetic Fields [36]:

$$\frac{\partial}{\partial x}\mathbf{v}(x,t)+\mathbf{L_G}\frac{\partial}{\partial t}\mathbf{i}(x,t)+\frac{\partial}{\partial t}\int_0^t \mathbf{r}'(t-\tau)\mathbf{i}(x,\tau)d\tau=\frac{\partial}{\partial t}\begin{bmatrix}\vdots\\ \int_0^{h_i}\overline{\mathcal{B}}^{inc}\cdot\hat{a}_n dl_i\\ \vdots\end{bmatrix} \tag{4.1}$$

$$\frac{\partial}{\partial x}\mathbf{i}(x,t)+\mathbf{C}\frac{\partial}{\partial t}\mathbf{v}(x,t)=-\mathbf{G}\begin{bmatrix}\vdots\\ \int_0^{h_i}\overline{\mathcal{E}}^{inc}\cdot\overline{dl_i}\\ \vdots\end{bmatrix}-\mathbf{C}\frac{\partial}{\partial t}\begin{bmatrix}\vdots\\ \int_0^{h_i}\overline{\mathcal{E}}^{inc}\cdot\overline{dl_i}\\ \vdots\end{bmatrix} \tag{4.2}$$

where $\mathbf{v}(x,t)$ and $\mathbf{i}(x,t)$ are the voltage and current vectors at any point along the line; $\mathbf{L_G}$, $\mathbf{C}$ and $\mathbf{G}$ are the per-unit-length geometric inductance, capacitance and conductance matrices respectively[25]; $\mathbf{r}'(t)$ is the transient resistance matrix[26]; $\overline{\mathcal{B}}^{inc}$ and $\overline{\mathcal{E}}^{inc}$ are the incident

magnetic field density and electric field intensity, respectively; $\hat{a}_n$ is the unit vector normal to the surface defined by the *i-th* conductor and the ground plane; $\overline{dl} = dl\,\hat{a}_l$ is the line differential of the integration trajectory from the earth plane to the *i-th* conductor. If the line has *n* conductors $\mathbf{L_G}$, **C** and **G** are of order *nxn*.

As presented in Chapter 2 the frequency domain version of **r'**(t), **R'**(s), can be calculated over any frequency range and then each one of its elements may be approximated by a rational function expanded in partial fractions as follows [27]:

$$R'_{ij} = \frac{1}{s}k_0 + k_\infty + \sum_{l=1}^{N}\frac{1}{s-p_l}k_l \tag{4.7}$$

Therefore, using the procedure presented in Chapter 2, (4.1) can be written as

$$\frac{\partial}{\partial x}\mathbf{v}(x,t) + \mathbf{L}_{cor}\frac{\partial}{\partial t}\mathbf{i}(x,t) + \mathbf{R}_{dc}\mathbf{i}(x,t) + \frac{\partial}{\partial t}\int_0^t \mathbf{h}(t-\tau)\mathbf{i}(x,\tau)d\tau = \frac{\partial}{\partial t}\begin{bmatrix} \vdots \\ \int_0^{h_i} \overline{\mathcal{B}}^{inc}\cdot\hat{a}_n dl_i \\ \vdots \end{bmatrix} \tag{4.13}$$

where:

$$\mathbf{L}_{cor} = \mathbf{L}_G + \mathbf{K}_\infty \tag{4.14a}$$

$$\mathbf{h}(t) = \sum_{l=1}^{N} e^{\mathbf{p}_l t}\mathbf{K}_l \tag{4.14b}$$

Equations (4.13) and (4.2) describe the electromagnetic behavior of an Overhead Multiconductor TL with frequency dependent electrical parameters excited by an external electromagnetic field.

4.3 YEE'S METHOD

The finite difference-time domain (FD-TD) also called Yee's Method is a technique that imposes a rectangular grid over the region of interest and solves a discretized version of the TL equations at the nodes of the grid [35].

Equations (4.13) and (4.2) can be ordered as follows:

$$\frac{\partial}{\partial t}\mathbf{v}(x,t) = \mathbf{C}^{-1}\left(\frac{\partial}{\partial t}\boldsymbol{\psi}^{\varepsilon} - \frac{\partial}{\partial \mathrm{x}}\mathbf{i}(x,t)\right) \tag{4.15}$$

$$\frac{\partial}{\partial t}\mathbf{i}(x,t) = \mathbf{L}_{cor}^{-1}\left(\frac{\partial}{\partial t}\boldsymbol{\psi}^{\mathcal{B}} - \frac{\partial}{\partial x}\mathbf{v}(x,t) - \mathbf{R}_{dc}\mathbf{i}(x,t) - \boldsymbol{\xi}(x,t)\right) \tag{4.16}$$

where

$$\boldsymbol{\xi}(x,t) = \frac{\partial}{\partial t}\left[\int_0^t \mathbf{h}(x,t-\tau)\mathbf{i}(x,\tau)d\tau\right] \tag{4.17a}$$

$$\boldsymbol{\psi}^{\mathcal{B}} = \begin{bmatrix} \vdots \\ \int_0^{h_i} \mathcal{B}_y^{inc} dx_i \\ \vdots \end{bmatrix} \quad \boldsymbol{\psi}^{\mathcal{E}} = -\mathrm{C}\begin{bmatrix} \vdots \\ \int_0^{h_i} \mathcal{E}_x^{inc} dx_i \\ \vdots \end{bmatrix} \tag{4.17b,c}$$

The vector $\boldsymbol{\xi}$ in (4.16) involves a convolution of the current $\mathbf{i}(x,t)$ with $\mathbf{h}(x,t)$. As it was presented in Chapter 2 the latter function can be expressed in the Laplace domain as a rational function expanded into partial fractions. Therefore the convolution term can be solved using a recursive scheme at each distance point x, as follows:

$$\boldsymbol{\xi}(d,t) = \frac{\partial}{\partial t}\boldsymbol{\gamma}(d,t) \cong \frac{1}{\Delta t}\left(\boldsymbol{\gamma}_d^{n+1} - \boldsymbol{\gamma}_d^{n}\right) \tag{4.24}$$

where the terms $\boldsymbol{\gamma}_d^n$ and $\boldsymbol{\gamma}_d^{n+1}$ are as defined in Chapter 2.

Equations (4.15) and (4.16) will be approximated using finite differences for the derivatives and linear interpolation where the values of voltages and currents are required. Fig.4.1 shows the grid used for this procedure. According to Fig. 4.1, approximating the derivatives in (4.15) and (4.16) with central differences gives:

$$\frac{\mathbf{v}_k^{n+1} - \mathbf{v}_k^{n}}{\Delta t} = \mathbf{C}_k^{-1}\left(\frac{\boldsymbol{\psi}_k^{\mathcal{E}n+1} - \boldsymbol{\psi}_k^{\mathcal{E}n}}{\Delta t} - \frac{\mathbf{i}_{k+1/2}^{n+1/2} - \mathbf{i}_{k-1/2}^{n+1/2}}{\Delta x}\right) \tag{4.25}$$

and

$$\frac{\mathbf{i}_{k+1/2}^{n+3/2} - \mathbf{i}_{k+1/2}^{n+1/2}}{\Delta t} = (\mathbf{L}_{cor,k+1/2})^{-1}\left[\frac{\boldsymbol{\psi}^{\mathcal{B}n+1} - \boldsymbol{\psi}^{\mathcal{B}n}}{\Delta t} - \frac{\mathbf{v}_{k+1}^{n+1} - \mathbf{v}_k^{n+1}}{\Delta x} - \mathbf{R}_{dc,k+1/2}\frac{\mathbf{i}_{k+1/2}^{n+3/2} + \mathbf{i}_{k+1/2}^{n+1/2}}{2} - \frac{\boldsymbol{\xi}^{n+1} + \boldsymbol{\xi}^{n}}{2}\right] \tag{4.26}$$

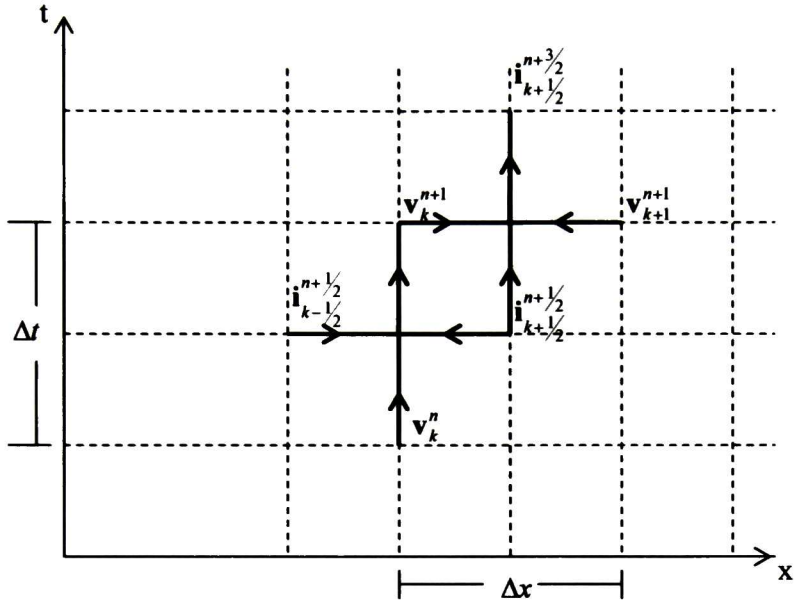

Fig.4.1. FD-TD grid

From (4.25) and (4.26) the following time-marching algorithm can be written

$$\mathbf{v}_k^{n+1} = \mathbf{v}_k^n + \mathbf{C}_k^{-1}\frac{\Delta t}{\Delta x}\left(\mathbf{C}_k^{-1}\frac{\Delta x}{\Delta t}\left(\boldsymbol{\psi}^{\varepsilon n+1} - \boldsymbol{\psi}^{\varepsilon n}\right) - \left(\mathbf{i}_{k+1/2}^{n+1/2} - \mathbf{i}_{k-1/2}^{n+1/2}\right)\right) \tag{4.27}$$

and

$$\begin{aligned}\mathbf{i}_{k+1/2}^{n+3/2} = \mathbf{H}_{k+1/2}&\left(\Delta t^{-1}\left(\sum_{l=1}^{N}\boldsymbol{\gamma}_{l,k+1/2}^{n} - \sum_{l=1}^{N}\left[1+\mathbf{p}_l\Delta t\right]^{-1}\boldsymbol{\gamma}_{l,k+1/2}^{n}\right) - \Delta x^{-1}\left(\mathbf{v}_{k+1}^{n+1} - \mathbf{v}_k^{n+1}\right)\right)\\ &+ \mathbf{H}_{k+1/2}\left(\left(\mathbf{L}_{cor,k+1/2}\Delta t^{-1} + \frac{\mathbf{R}_{dc,k+1/2}}{2}\right)\mathbf{i}_{k+1/2}^{n+1/2} + \Delta t^{-1}\left(\boldsymbol{\psi}^{\mathcal{B}n+1} - \boldsymbol{\psi}^{\mathcal{B}n}\right)\right)\end{aligned} \tag{4.28}$$

where

$$\mathbf{H}_{k+1/2} = \left(\mathbf{L}_{cor,k+1/2}\Delta t^{-1} + \frac{\mathbf{R}_{dc,k+1/2}}{2} + \sum_{l=1}^{N}\mathbf{K}_l\left[1+\mathbf{p}_l\Delta t\right]^{-1}\right)^{-1} \tag{4.29}$$

Superscripts *"n"* and *"n+1/2"* indicate any time step while *"n+1"* and *"n+3/2"* indicate the next time step for the voltage and current vectors respectively. Subscripts *k* and *k+1/2* indicate the position where each quantity is calculated, as shown in Fig.4.1.

4.4 BOUNDARY CONDITIONS

Consider a section of the grid at x = 0, as shown in Fig. 4.2. Using central differences for the time derivatives and forward differences for the space derivatives in (4.15):

$$\frac{\mathbf{v}_0^{n+1}-\mathbf{v}_0^{n}}{\Delta t}=\mathbf{C}_0^{-1}\left[\frac{\boldsymbol{\psi}^{\varepsilon n+1}-\boldsymbol{\psi}^{\varepsilon n}}{\Delta t}-\frac{\mathbf{i}_{1/2}^{n+1/2}-\mathbf{i}_0^{n+1/2}}{\Delta x/2}\right] \tag{4.30}$$

Current $\mathbf{i}_0^{n+1/2}$ is unknown but it can be approximated by interpolation as follows

$$\mathbf{i}_0^{n+1/2}=\frac{\mathbf{i}_0^{n+1}+\mathbf{i}_0^{n}}{2} \tag{4.31}$$

Substituting (4.31) into (4.30)

$$\mathbf{v}_0^{n+1}=\mathbf{v}_0^{n}+\left(\frac{\Delta t\mathbf{C}_0^{-1}}{\Delta x}\right)\mathbf{i}_0^{n+1}+\left(\frac{\Delta t\mathbf{C}_0^{-1}}{\Delta x}\right)\left(\mathbf{i}_0^{n}-2\mathbf{i}_1^{n+1/2}\right)+\mathbf{C}_0^{-1}\left(\boldsymbol{\psi}^{\varepsilon n+1}-\boldsymbol{\psi}^{\varepsilon n}\right) \tag{4.30}$$

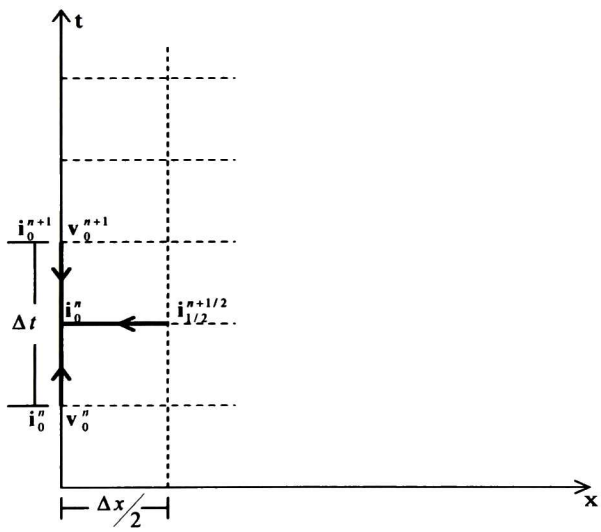

Fig.4.2. Voltages and current at the sending end for the grid of Yee's method.

Rearranging (4.30) it can be written:

$$\mathbf{i}_0^{n+1}=\mathbf{Y}_e\mathbf{v}_0^{n+1}+\mathbf{i}_{hist1} \tag{4.31}$$

where

$$\mathbf{Y}_e = \left(\frac{\Delta x}{\Delta t}\right)\mathbf{C}_0 \tag{4.32a}$$

$$\mathbf{i}_{histe} = \left(2\mathbf{i}_{1/2}^{n+1/2} - \mathbf{i}_0^n\right) - \mathbf{Y}_e\mathbf{v}_0^n - \left(\frac{\Delta x}{\Delta t}\right)\left(\boldsymbol{\psi}^{\varepsilon n+1} - \boldsymbol{\psi}^{\varepsilon n}\right) \tag{4.32b}$$

In a similar way consider now a portion of the grid near x = L, as shown in Fig. 4.3. At the receiving end we have the following approximation:

$$\frac{\mathbf{v}_l^{n+1} - \mathbf{v}_l^n}{\Delta t} = \mathbf{C}_l^{-1}\left[\frac{\boldsymbol{\psi}^{\varepsilon n+1} - \boldsymbol{\psi}^{\varepsilon n}}{\Delta t} - \frac{\mathbf{i}_l^{n+1/2} - \mathbf{i}_{l-1/2}^{n+1/2}}{\Delta x/2}\right] \tag{4.33}$$

and

$$\mathbf{i}_l^{n+1/2} = \frac{\mathbf{i}_l^{n+1} + \mathbf{i}_l^n}{2} \tag{4.34}$$

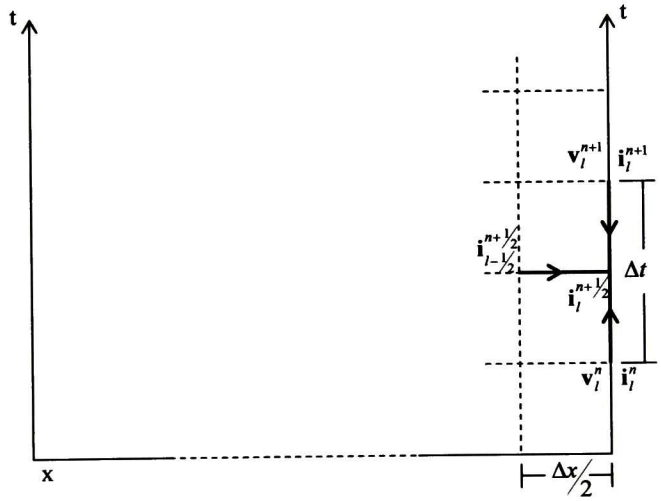

Fig.4.3. Voltages and current at the receiving end Yee's mesh.

Substituting (4.34) in (4.33)

$$\mathbf{v}_l^{n+1} = \mathbf{v}_l^n - \left(\frac{\Delta t\mathbf{C}_l^{-1}}{\Delta x}\right)\mathbf{i}_l^{n+1} + \left(\frac{\Delta t\mathbf{C}_l^{-1}}{\Delta x}\right)\left(2\mathbf{i}_{l-1/2}^{n+1/2} - \mathbf{i}_l^n\right) + \mathbf{C}_l^{-1}\left(\boldsymbol{\psi}^{\varepsilon n+1} - \boldsymbol{\psi}^{\varepsilon n}\right) \tag{4.35}$$

After some algebraic manipulations, (4.35) can be written as follows:

$$\mathbf{i}_l^{n+1} = \mathbf{Y}_r\mathbf{v}_l^{n+1} + \mathbf{i}_{hist2} \tag{4.36}$$

where

$$\mathbf{Y}_r = \mathbf{C}_l \frac{\Delta x}{\Delta t} \tag{4.37a}$$

$$\mathbf{i}_{histr} = \left(\mathbf{i}_l^n - 2\mathbf{i}_{l-1/2}^{n+1/2}\right) - \mathbf{Y}_r \mathbf{v}_l^n + \frac{\Delta x}{\Delta t}\left(\psi^{\varepsilon n+1} - \psi^{\varepsilon n}\right) \tag{4.37b}$$

Equations (4.31) and (4.36) represent Norton models for the transmission line ends, as shown in Fig.4.4. Current sources $\mathbf{i}_{hist1}$ and $\mathbf{i}_{hist2}$ at any time step t are given in terms of voltages and currents calculated at time t-Δt and t-$\Delta t/2$ respectively at the first and last interior points.

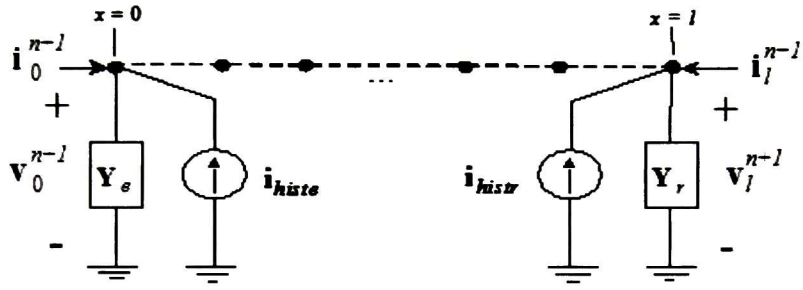

Fig.4.4. Norton equivalent circuit for the transmission line ends based on Yee's Method.

4.5 APPLICATION EXAMPLES

a) As an application example consider example a) of Chapter 3. For the shake of completeness data for this example is repeated here (see Fig.4.5). The line is formed by parallel conductors with 2.54 cm of radius and 10 m of horizontal separation; the ground resistivity is assumed to be 100 Ω-m. A unit step voltages was applied to the conductors at the sending end and the receiving end was left open. Source resistances of 10 Ω were used.

The number of line segments in cascade connection for the EMTP and Yee's Method was 20. In order to take into account the frequency dependence of the electrical parameters in the EMTP the J. Marti model was used. Figure 4.6 shows the voltages at phase C of the receiving node obtained with both methods.

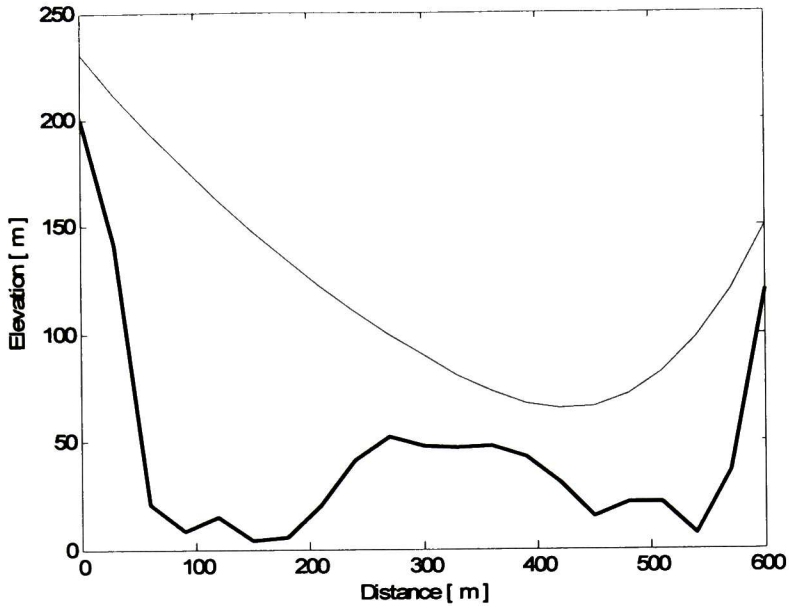

Fig.4.5. Nonuniform Transmission Line geometry

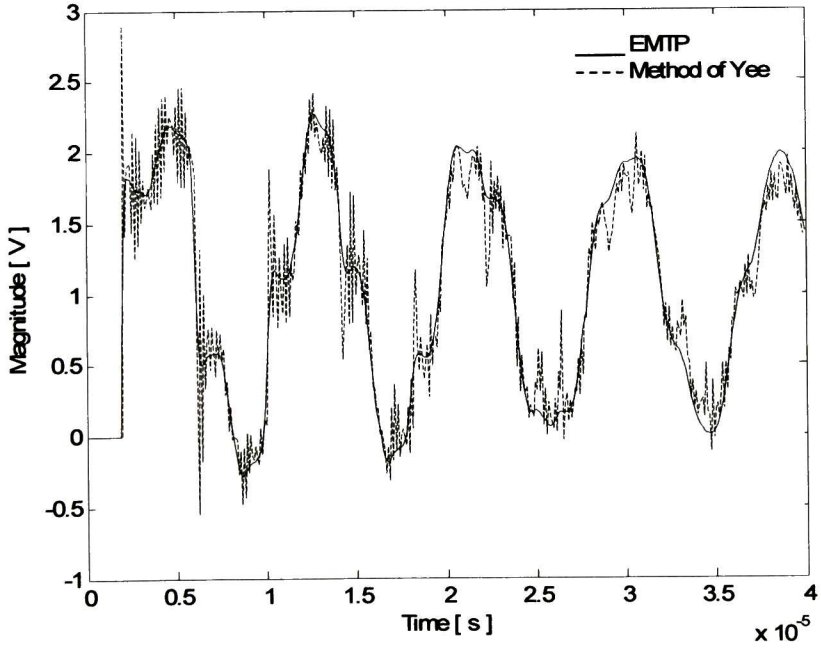

Fig.4.6. Waveform voltages at the receiving end phase C. EMTP against Method of Yee.

b) As a second example consider a three-phase transmission line excited by an Electromagnetic plane wave. The data of the line are the following: length 325m, conductors radius 2.54 cm and ground resistivity of 100 Ωm. The geometry of the line is shown in Fig.4.7. At the sending end loads of 200 Ω are connected and at the receiving end the conductors are open ended. The electric and magnetic fields vary only with respect to time as shown in Fig.4.8 and Fig.4.9.

Figure 4.10 shows the voltage waveforms obtained at both ends on phase C. For both methods the line was subdivided in 25 sections of length Δx =13m. To obtain the voltage waveforms using EMTP, the incident field effects were included by inserting equivalent current sources between line subsections.

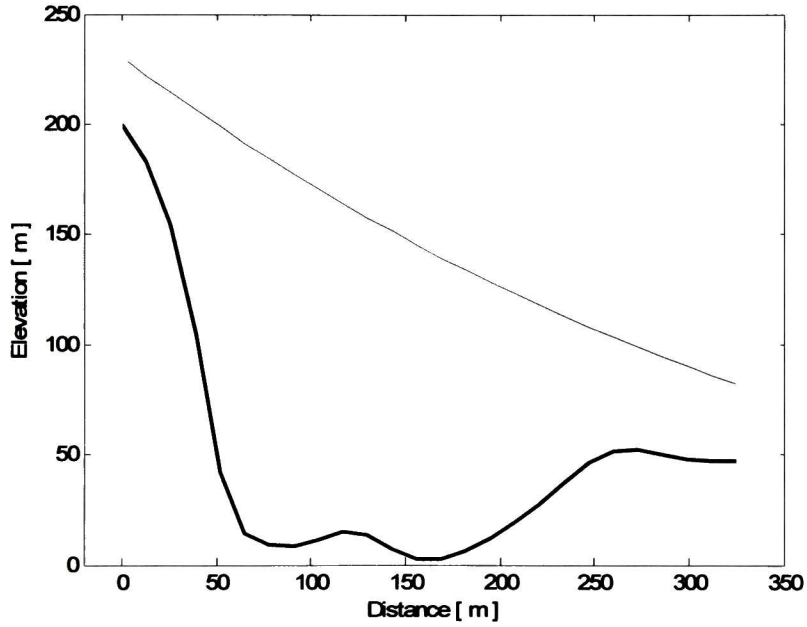

Fig.4.7.Nonuniform three phase Transmission Line geometry

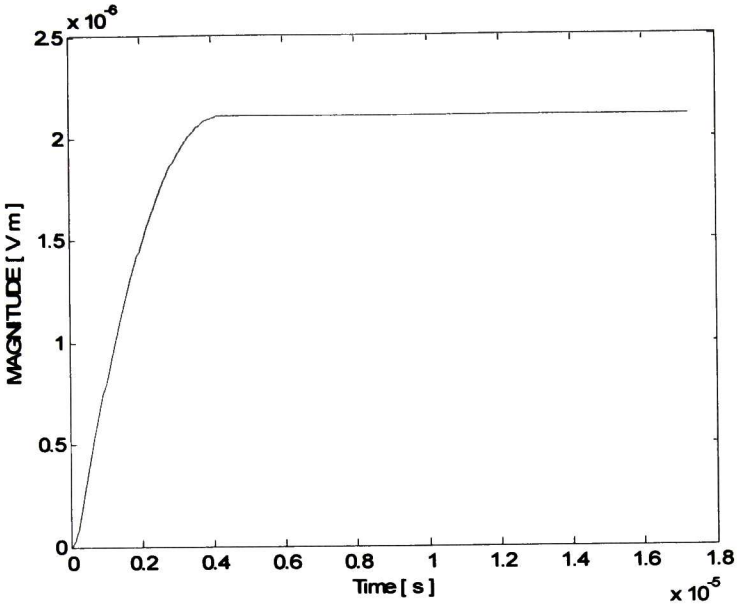

Fig.4.8. Incident Electric Field

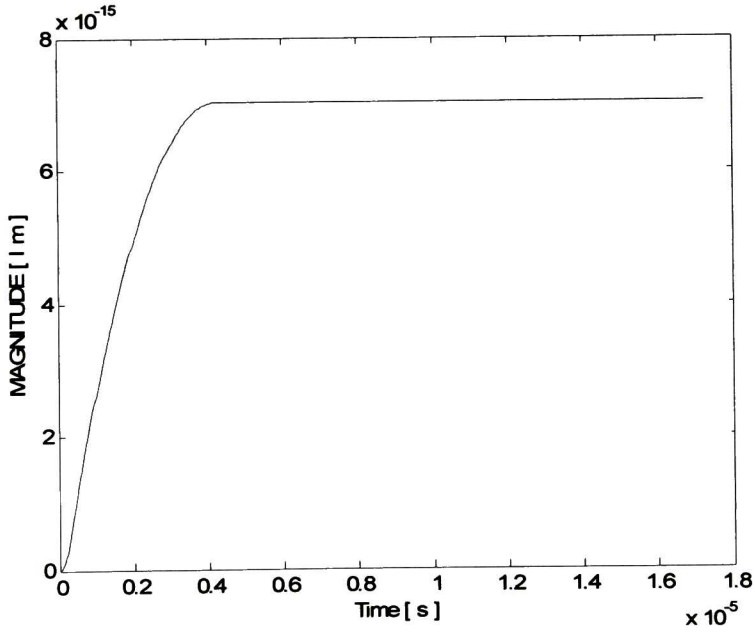

Fig.4.9. Incident Magnetic Field

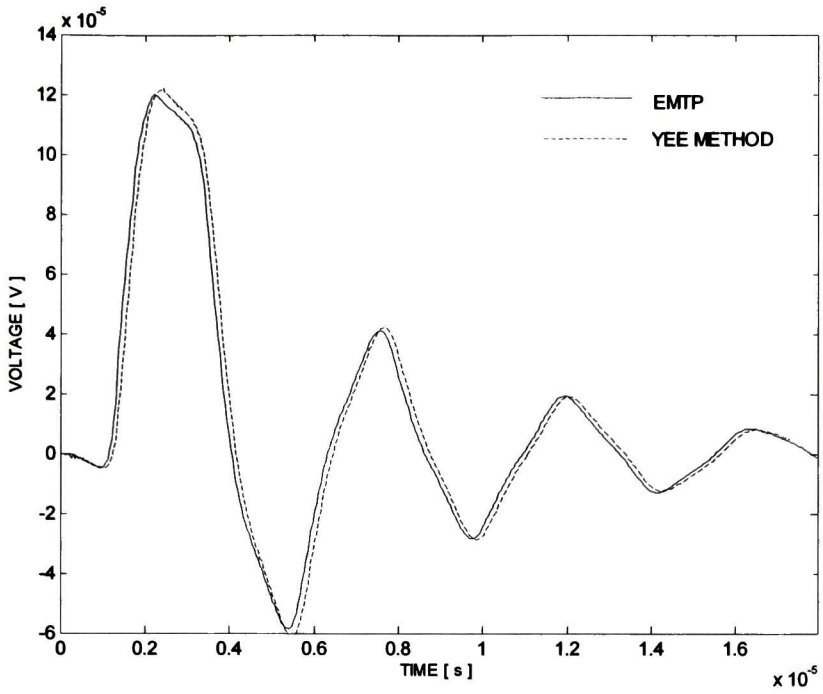

Fig.4.10. Waveforms Voltage at the sending end phase C. EMTP against Method of Yee

4.6 OBSERVATIONS

The results obtained show that the FDTD method produces numerical oscillations for the case where the excitation is injected at the transmission line ends [25]. However as shown in the second example for the case of incident field excitation the numerical oscillations are minimum or imperceptible.

5 THE METHOD OF CHARACTERISTICS FOR FIELD EXCITED NONUNIFORM MULTICONDUCTOR TRANSMISSION LINES

5.1 INTRODUCTION

In this chapter the Method of Characteristics developed in Chapter 3 is extended to the problem of field excited Multiconductor Transmission Lines. The incident fields may be in the form of uniform plane waves such as those generated by distant transmitting antennas or they may be nonuniform fields such as those generated by nearby radiating structures and lightning.

5.2 METHOD OF CHARACTERISTICS

The telegrapher's equations, as shown in Chapter 4, for the case of field excited multiconductor transmission lines are:

$$\frac{\partial}{\partial x}\mathbf{v}(x,t)+\mathbf{L}_{cor}\frac{\partial}{\partial t}\mathbf{i}(x,t)+\mathbf{R}_{dc}\mathbf{i}(x,t)+\frac{\partial}{\partial t}\int_0^t \mathbf{h}(t-\tau)\mathbf{i}(x,\tau)d\tau=\frac{\partial}{\partial t}\begin{bmatrix}\vdots\\ \int_0^{h_i}\overline{\mathcal{B}}^{inc}\cdot\hat{a}_n dl_i\\ \vdots\end{bmatrix} \tag{5.1}$$

$$\frac{\partial}{\partial x}\mathbf{i}(x,t)+\mathbf{C}\frac{\partial}{\partial t}\mathbf{v}(x,t)=-\mathbf{G}\begin{bmatrix}\vdots\\ \int_0^{h_i}\overline{\mathcal{E}}^{inc}\cdot\overline{dl_i}\\ \vdots\end{bmatrix}-\mathbf{C}\frac{\partial}{\partial t}\begin{bmatrix}\vdots\\ \int_0^{h_i}\overline{\mathcal{E}}^{inc}\cdot\overline{dl_i}\\ \vdots\end{bmatrix} \tag{5.2}$$

where:

$$\mathbf{L}_{cor}=\mathbf{L}_G+\mathbf{K}_\infty \tag{5.14a}$$

$$\mathbf{h}(t)=\sum_{l=1}^{N}e^{\mathbf{p}_l t}\mathbf{K}_l \tag{5.14b}$$

Expressions (5.1) and (5.2) can compactly be expressed as follows to get a $2n$ first order differential equations system with x and t as independent variables.

$$\frac{\partial}{\partial t}\mathbf{U}+\mathbf{A}\frac{\partial}{\partial x}\mathbf{U}+\mathbf{B}\mathbf{U}-\mathbf{A}\frac{\partial}{\partial t}\mathbf{E}+\mathbf{f}=\mathbf{0} \tag{5.15}$$

where:

$$\mathbf{U}=\begin{bmatrix}\mathbf{v}(x,t)\\ \mathbf{i}(x,t)\end{bmatrix} \tag{5.16a}$$

$$\mathbf{A}=\begin{bmatrix}0 & \mathbf{C}^{-1}(x)\\ \mathbf{L}_{cor}^{-1}(x) & 0\end{bmatrix} \tag{5.16b}$$

$$\mathbf{B}=\begin{bmatrix}\mathbf{0} & \mathbf{0}\\ \mathbf{0} & \mathbf{L}_{cor}^{-1}(x)\mathbf{R}_{dc}(x)\end{bmatrix} \tag{5.16c}$$

$$\mathbf{f}=\begin{bmatrix}\mathbf{0}\\ \mathbf{L}_{cor}^{-1}(x)\boldsymbol{\xi}(x,t)\end{bmatrix} \tag{5.16d}$$

$$\mathbf{E}=\begin{bmatrix}\boldsymbol{\psi}^{\mathcal{B}}\\ \boldsymbol{\psi}^{\mathcal{E}}\end{bmatrix} \tag{5.16e}$$

and

$$\boldsymbol{\xi}(x,t)=\frac{\partial}{\partial t}\left[\int_0^t \mathbf{h}(x,t-\tau)\mathbf{i}(x,\tau)d\tau\right] \tag{5.17a}$$

$$\boldsymbol{\psi}^{\mathcal{B}}=\begin{bmatrix}\vdots\\ \int_0^{h_i}\mathcal{B}_y^{inc}dx_i\\ \vdots\end{bmatrix} \tag{5.17b}$$

$$\boldsymbol{\psi}^{\mathcal{E}}=-\mathrm{C}\begin{bmatrix}\vdots\\ \int_0^{h_i}\mathcal{E}_x^{inc}dx_i\\ \vdots\end{bmatrix} \tag{5.17c}$$

Using the definitions of eigenvalues and eigenvectors and the procedure introduced in Chapter 3 expression (5.15) can be transformed into the following pair of equations:

$$\left(\frac{\partial \mathbf{v}_m}{\partial t}+\mathbf{\Phi}\frac{\partial \mathbf{v}_m}{\partial x}\right)+\mathbf{Z}_{\mathrm{W}}\left(\frac{\partial \mathbf{i}_m}{\partial t}+\mathbf{\Phi}\frac{\partial \mathbf{i}_m}{\partial x}\right)+\mathbf{\Phi}\mathbf{R}_m\mathbf{i}_m+\mathbf{\Phi}\mathbf{T}_{\mathrm{v}}^{-1}\boldsymbol{\xi}-\mathbf{Z}_{\mathrm{W}}\mathbf{\Phi}\frac{\partial}{\partial t}\boldsymbol{\psi}_m^{\mathcal{E}}-\mathbf{\Phi}\frac{\partial}{\partial t}\boldsymbol{\psi}_m^{\mathcal{B}}=\mathbf{0} \tag{5.23a}$$

$$\left(\frac{\partial \mathbf{v}_m}{\partial t}-\mathbf{\Phi}\frac{\partial \mathbf{v}_m}{\partial x}\right)-\mathbf{Z}_{\mathrm{W}}\left(\frac{\partial \mathbf{i}_m}{\partial t}-\mathbf{\Phi}\frac{\partial \mathbf{i}_m}{\partial x}\right)-\mathbf{\Phi}\mathbf{R}_m\mathbf{i}_m-\mathbf{\Phi}\mathbf{T}_{\mathrm{v}}^{-1}\boldsymbol{\xi}-\mathbf{Z}_{\mathrm{W}}\mathbf{\Phi}\frac{\partial}{\partial t}\boldsymbol{\psi}_m^{\mathcal{E}}+\mathbf{\Phi}\frac{\partial}{\partial t}\boldsymbol{\psi}_m^{\mathcal{B}}=\mathbf{0} \tag{5.23b}$$

where $\mathbf{v}_m$ and $\mathbf{i}_m$ are modal vectors of voltage and current and $\boldsymbol{\psi}_m^{\mathcal{B}}$ and $\boldsymbol{\psi}_m^{\mathcal{E}}$ are the modal quantities corresponding to $\boldsymbol{\psi}^{\mathcal{B}}$ and $\boldsymbol{\psi}^{\mathcal{E}}$ defined by

$$\mathbf{v}_m=\mathbf{T}_{\mathrm{V}}^{-1}\mathbf{v}(x,t) \tag{5.24a}$$

$$\mathbf{i}_m=\mathbf{T}_{\mathrm{I}}^{-1}\mathbf{i}(x,t) \tag{5.24b}$$

$$\boldsymbol{\psi}_m^{\mathcal{B}}=\mathbf{T}_{\mathrm{V}}^{-1}\boldsymbol{\psi}^{\mathcal{B}} \tag{5.25a}$$

$$\boldsymbol{\psi}_m^{\mathcal{E}}=\mathbf{T}_{\mathrm{I}}^{-1}\boldsymbol{\psi}^{\mathcal{E}} \tag{5.25b}$$

and $\mathbf{R}_m$ is a nondiagonal modal resistance matrix given by

$$\mathbf{R}_m=\mathbf{T}_{\mathrm{V}}^{-1}\mathbf{R}_{dc}\mathbf{T}_{\mathrm{I}} \tag{5.26}$$

Consider now the curves on the *x-t* plane defined by the following differential equations:

$$\phi_j=\pm\frac{dx_j}{dt} \qquad j=1,\ldots\ldots,n \tag{5.27}$$

where the plus sign corresponds to (5.23a) and the minus sign to (5.23b). Solutions to (5.27) are known as *characteristics* and represent a new coordinates system for equations (5.23). In the case of NU lines (5.27) defines curves with distance dependent positive or negative derivatives. However, as presented in Chapter 3 for a piece-wise uniform transmission line the characteristics are families of straight lines.

When (5.27) holds, equations (5.23) become:

$$\frac{d\mathbf{v}_m}{dt} + \mathbf{Z}_w \frac{d\mathbf{i}_m}{dt} + \frac{d\mathbf{X}}{dt}\mathbf{R}_m\mathbf{i}_m + \frac{d\mathbf{X}}{dt}\mathbf{T}_V^{-1}\boldsymbol{\xi} - \mathbf{Z}_w \frac{d\mathbf{X}}{dt}\frac{\partial}{\partial t}\boldsymbol{\psi}_{mj}^{\mathcal{E}} - \frac{d\mathbf{X}}{dt}\frac{\partial}{\partial t}\boldsymbol{\psi}_{mj}^{\mathcal{B}} = \mathbf{0} \qquad (5.28a)$$

$$\frac{d\mathbf{v}_m}{dt} - \mathbf{Z}_w \frac{d\mathbf{i}_m}{dt} + \frac{d\mathbf{X}}{dt}\mathbf{R}_m\mathbf{i}_m + \frac{d\mathbf{X}}{dt}\mathbf{T}_V^{-1}\boldsymbol{\xi} + \mathbf{Z}_w \frac{d\mathbf{X}}{dt}\frac{\partial}{\partial t}\boldsymbol{\psi}_{mj}^{\mathcal{E}} - \frac{d\mathbf{X}}{dt}\frac{\partial}{\partial t}\boldsymbol{\psi}_{mj}^{\mathcal{B}} = \mathbf{0} \qquad (5.28b)$$

where

$$\frac{d\mathbf{X}}{dt} = diag\left(\frac{dx_j}{dt}\right) \qquad j = 1,\ldots\ldots,n \qquad (5.29)$$

The vector ξ in (5.28) involves a convolution of the current $\mathbf{i}(x,t)$ with $\mathbf{h}(x,t)$. The latter function can be expressed in the Laplace domain as a rational function expanded into partial fractions and then it can be solved using a recursive scheme as was shown in Chapter 2.

5.3 NUMERICAL SOLUTION

Equation (5.28) can be approximated using finite differences. Fig. 5.1 shows a graphical interpretation of the characteristic curves of (5.27) that cross through point E at time $t=T+\Delta t$. By defining $\Delta x=max(\phi)\Delta t$ for the grid and $\Delta x_j=\phi_j\Delta t$ for each mode, the grid satisfies the Courant-Friedrichs-Lewy condition for the whole set of modes [32,33].

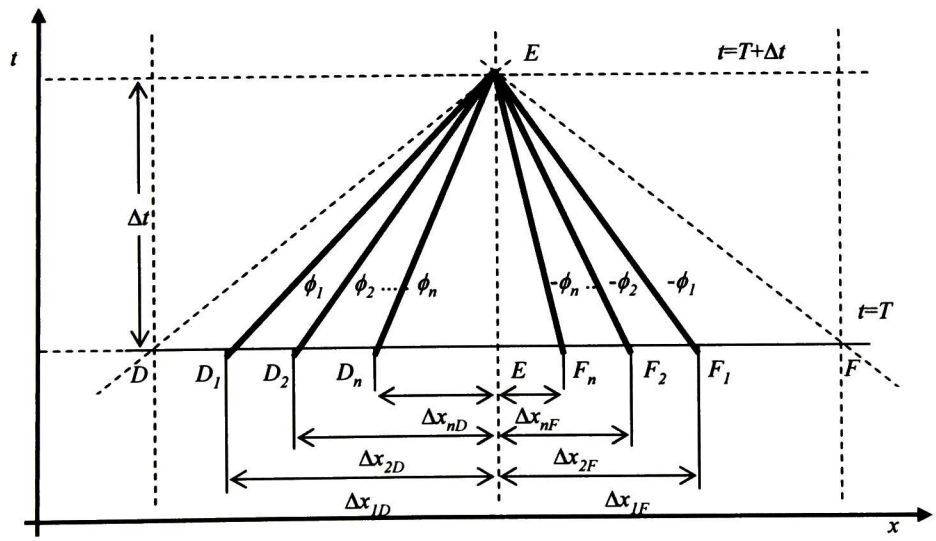

Fig.5.1. Characteristics in the x-t plane

Using finite differences to approximate the derivatives in (5.28) and averages for the required quantities at the evaluation points inside the line, as shown in Fig. 5.1, it can be written:

$$\begin{bmatrix} \mathbf{Y}_r & \mathbf{U} \\ \mathbf{Y}_e & -\mathbf{U} \end{bmatrix} \begin{bmatrix} \mathbf{v}_e^{n+1} \\ \mathbf{i}_e^{n+1} \end{bmatrix} = \begin{bmatrix} \mathbf{i}_{histr} \\ \mathbf{i}_{histe} \end{bmatrix} \tag{5.39}$$

where:

$$\mathbf{Y}_r = \mathbf{T}_{ID}\left(\mathbf{Z}_{WD} + \frac{\Delta \mathbf{x}}{2}\mathbf{R}_{mD} + \Delta \mathbf{x}\mathbf{T}_{VD}^{-1}\boldsymbol{\Psi}_D\mathbf{T}_{ID} \right)^{-1} \mathbf{T}_{VD}^{-1} \tag{5.40}$$

$$\mathbf{i}_{histr} = \mathbf{T}_{ID}\left(\mathbf{Z}_{WD} + \frac{\Delta \mathbf{x}}{2}\mathbf{R}_{mD} + \Delta \mathbf{x}\mathbf{T}_{VD}^{-1}\boldsymbol{\Psi}_D\mathbf{T}_{ID} \right)^{-1} \mathbf{T}_{VD}^{-1}\mathbf{v}_{histD} \tag{5.41}$$

$$\mathbf{Y}_e = \mathbf{T}_{IF}\left(\mathbf{Z}_{WF} + \frac{\Delta \mathbf{x}}{2}\mathbf{R}_{mF} + \Delta \mathbf{x}\mathbf{T}_{VF}^{-1}\boldsymbol{\Psi}_F\mathbf{T}_{IF} \right)^{-1} \mathbf{T}_{VF}^{-1} \tag{5.42}$$

$$\mathbf{i}_{histe} = \mathbf{T}_{IF}\left(\mathbf{Z}_{WF} + \frac{\Delta \mathbf{x}}{2}\mathbf{R}_{mF} + \Delta \mathbf{x}\mathbf{T}_{VF}^{-1}\boldsymbol{\Psi}_F\mathbf{T}_{IF} \right)^{-1} \mathbf{T}_{VF}^{-1}\mathbf{v}_{histF} \tag{5.43}$$

$$\mathbf{v}_e^{n+1} = \mathbf{T}_{VE}\mathbf{v}_{mE}^{n+1} \tag{5.44}$$

$$\mathbf{i}_e^{n+1} = \mathbf{T}_{IE}\mathbf{i}_{mE}^{n+1} \tag{5.45}$$

$$\Delta \mathbf{x} = diag(\Delta x_1, \Delta x_2, ..., \Delta x_n) \tag{5.46}$$

$$\boldsymbol{\Psi}_{D,F} = \sum_{l=1}^{N} \mathbf{K}_{lD,F}\left(1 + \mathbf{p}_{lD,F}\Delta t\right)^{-1} \tag{5.47}$$

being **U** the identity matrix and

$$\mathbf{v}_{histD} = \mathbf{T}_{VD}\left(\mathbf{v}_{mD}^{n} + \left[\mathbf{Z}_{WD} - \frac{\Delta \mathbf{x}}{2}\mathbf{R}_{mD} \right]\mathbf{i}_{mD}^{n} + \frac{\Delta \mathbf{x}}{\Delta t}\mathbf{T}_{VD}^{-1}\sum_{l=1}^{N}\boldsymbol{\gamma}'_{mDl} - \frac{\Delta \mathbf{x}}{\Delta t}\mathbf{T}_{VD}^{-1}\sum_{l=1}^{N}\left[1 + \mathbf{p}_l\Delta t\right]^{-1}\boldsymbol{\gamma}'_{mDl} \right)$$
$$+ \mathbf{T}_{VD}\frac{\Delta \mathbf{x}}{\Delta t}\left(\mathbf{Z}_{WD}\left(\boldsymbol{\psi}_{mE}^{\mathcal{E}n+1} - \boldsymbol{\psi}_{mD}^{\mathcal{E}n} \right) + \left(\boldsymbol{\psi}_{mE}^{\mathcal{B}n+1} - \boldsymbol{\psi}_{mD}^{\mathcal{B}n} \right) \right) \tag{5.46}$$

$$\mathbf{v}_{histF} = \mathbf{T}_{VF}\left(\mathbf{v}_{mF}^{n} - \left[\mathbf{Z}_{WF} - \frac{\Delta \mathbf{x}}{2}\mathbf{R}_{mF} \right]\mathbf{i}_{mF}^{n} - \frac{\Delta \mathbf{x}}{\Delta t}\mathbf{T}_{VF}^{-1}\sum_{l=1}^{N}\boldsymbol{\gamma}_{mFl}^{n} + \frac{\Delta \mathbf{x}}{\Delta t}\mathbf{T}_{VF}^{-1}\sum_{l=1}^{N}\left[1 + \mathbf{p}_l\Delta t\right]^{-1}\boldsymbol{\gamma}_{mFl}^{n} \right)$$
$$+ \mathbf{T}_{VF}\frac{\Delta \mathbf{x}}{\Delta t}\left(\mathbf{Z}_{WF}\left(\boldsymbol{\psi}_{mE}^{\mathcal{E}n+1} - \boldsymbol{\psi}_{mF}^{\mathcal{E}n} \right) + \left(\boldsymbol{\psi}_{mE}^{\mathcal{B}n} - \boldsymbol{\psi}_{mF}^{\mathcal{B}n+1} \right) \right) \tag{5.47}$$

the subscript "*n*" indicates any time step and "*n+1*" indicates the next time step. The letters *D*, *E*, and *F* in the subscripts indicate the position at which quantities are calculated, as shown in Fig.5.1. By solving (5.39) voltages and currents at point E at time $t=T+\Delta t$ can be found when voltages and currents at time $t=T$ are known.

5.4 BOUNDARY CONDITIONS

At the sending end of the line there exist only *n* characteristic curves, which correspond to equation (5.28b), as shown in Fig.5.2. Using the second row of equation (5.39):

$$\mathbf{i}_e^{n+1} = \mathbf{Y}_e \mathbf{v}_e^{n+1} - \mathbf{i}_{histe} \tag{5.42}$$

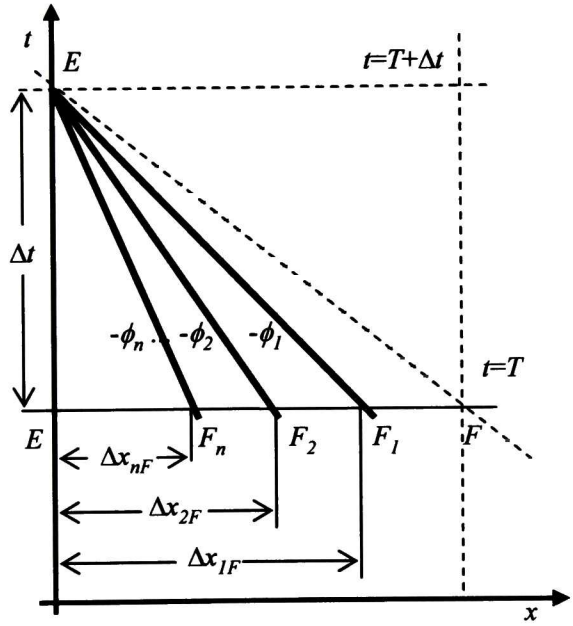

Fig.5.2. Characteristics curves at the sending end of the transmission line.

At the receiving end there exist only the *n* characteristics corresponding to (5.28b) as shown in Fig.5.3. From the first row of (5.52):

$$\mathbf{i}_r^{n+1} = \mathbf{Y}_r \mathbf{v}_r^{n+1} - \mathbf{i}_{histr} \tag{5.56}$$

where:

$$\mathbf{v}_r^{n+1} = \mathbf{v}_e^{n+1} \tag{5.57a}$$

$$\mathbf{i}_r^{n+1} = -\mathbf{i}_e^{n+1} \tag{5.57b}$$

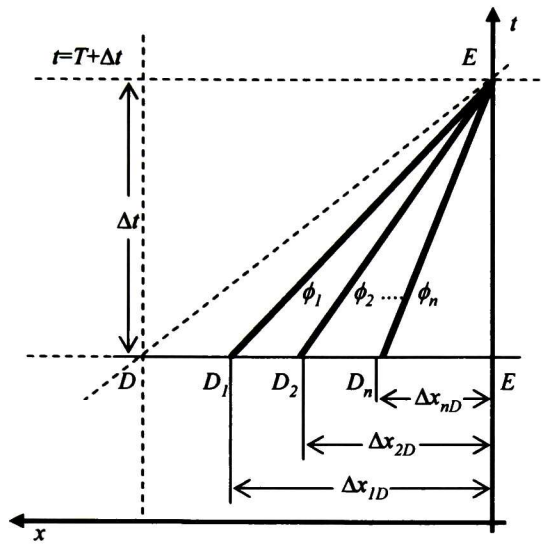

Fig.5.3. Characteristics curves at the receiving end of the transmission line

Equations (5.44) and (5.47) represent a Norton model for the transmission line ends, as shown in Fig.5.4. Current sources $\mathbf{i}_{histe}$ and $\mathbf{i}_{histr}$ at any time step t are given in terms of voltages and currents and the electric and magnetic effects from any external fields calculated at time t-Δt at the first and last interior points. Therefore at time t the transmission line ends are topologically disconnected.

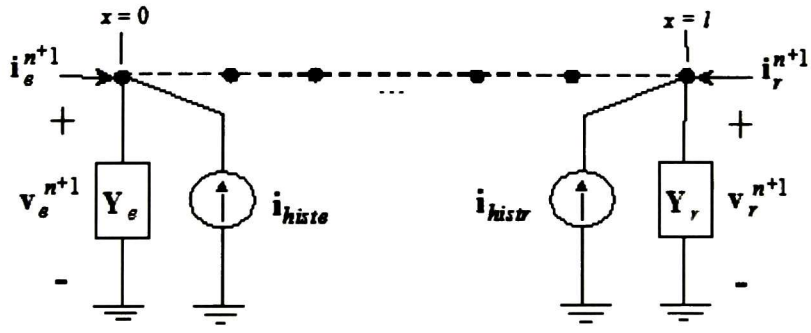

Fig.5.4. Norton equivalent circuits for the transmission line at the ends taking account the electric and magnetic external fields.

5.5 APPLICATIONS EXAMPLE

As an example, consider a Nonuniform three phase transmission Line which is hit by a uniform plane wave. The data of the line are: length of 325 m, the conductor radius is 2.54 cm and ground resistivity is 100 Ωm. The geometry of the line is shown in Fig.5.5. At the sending end of the TL a load of 200 Ω is connected and the receiving end left open. The incident Electric and Magnetic field are shown in Fig.5.6 and 5.7.

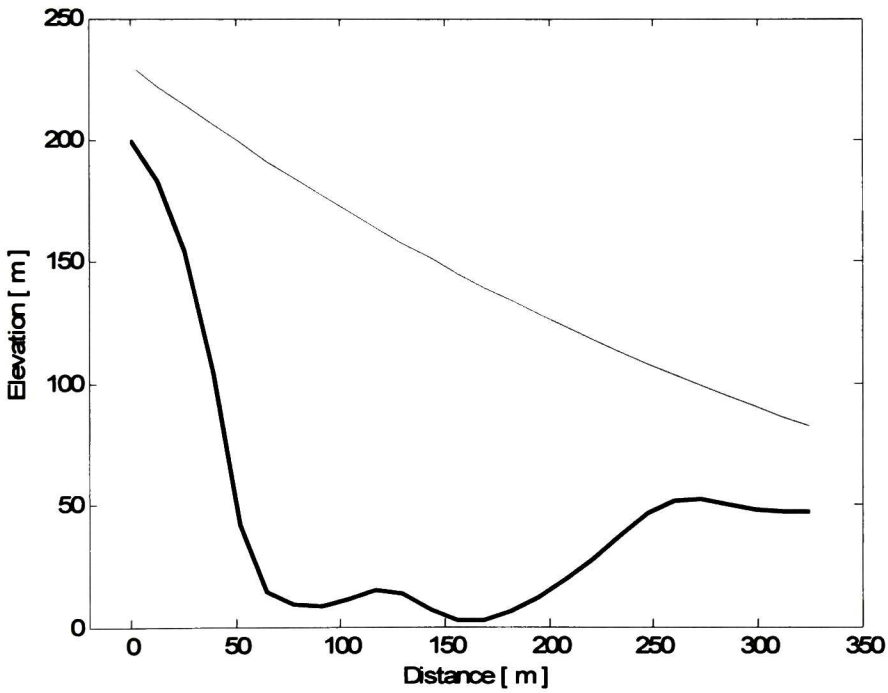

Fig.5.5. Nonuniform Line geometry.

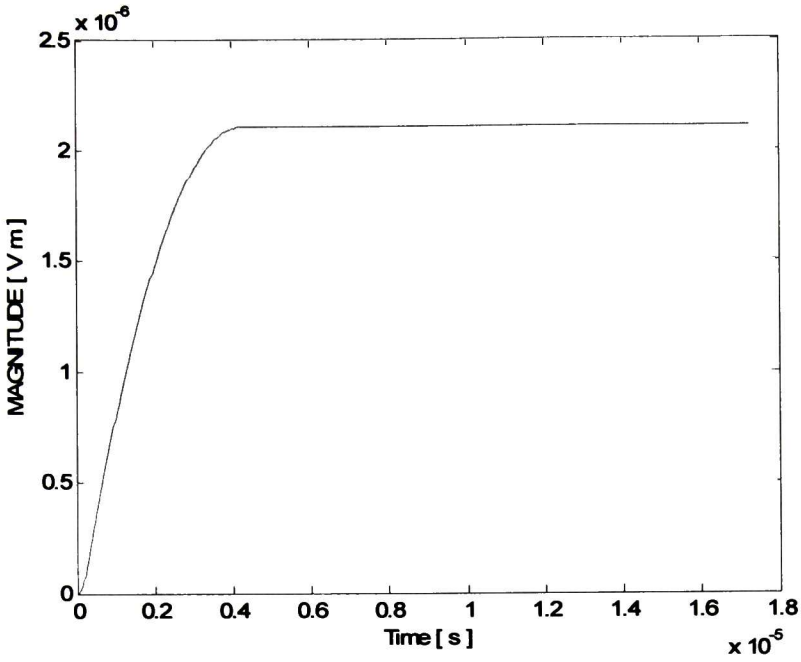

Fig.5.6. Electric field waveform.

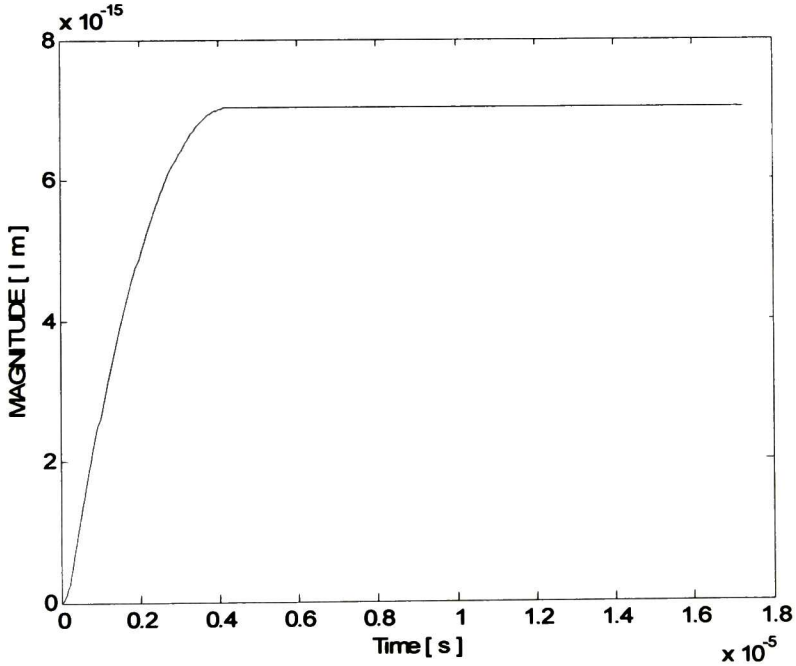

Fig.5.7. Magnetic field waveform.

Figure 5.8 shows voltages waveform at the sending end (and receiving end) with the Method of Characteristics and Yee's Method while Fig. 5.9 presents voltage waveforms at the sending end (and receiving end) for the EMTP and the Method of Characteristics. For the three simulations the line was subdivided into 25 sections of Δx=13m. As can be seen from the figures the three procedures provide almost the same results.

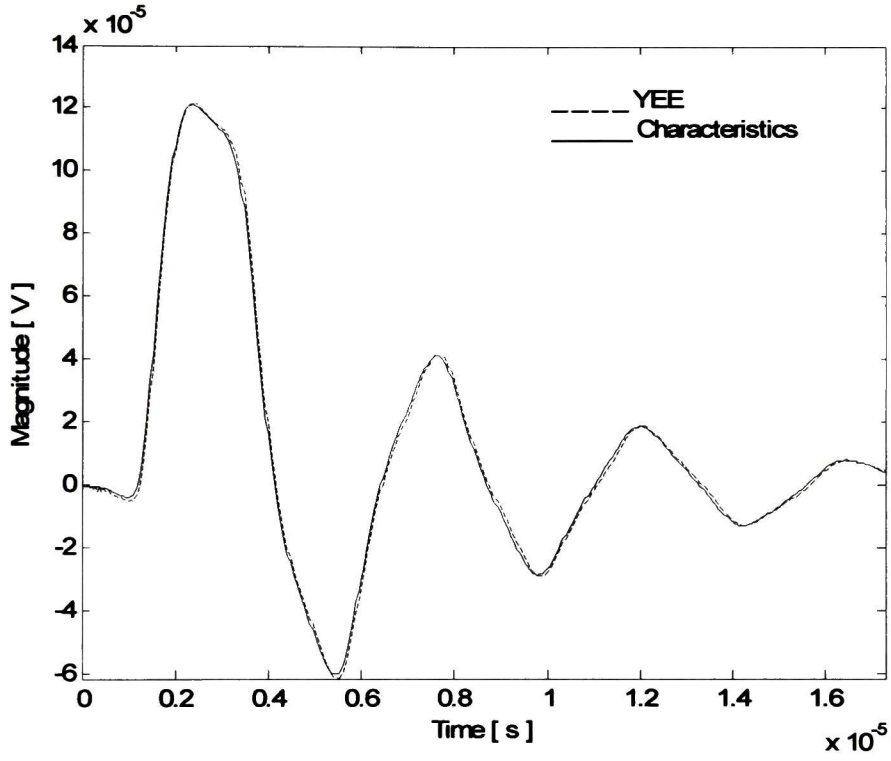

Fig.5.8. Voltages waveform at the sending end (and receiving end) with the Method of Characteristics and Yee's Method

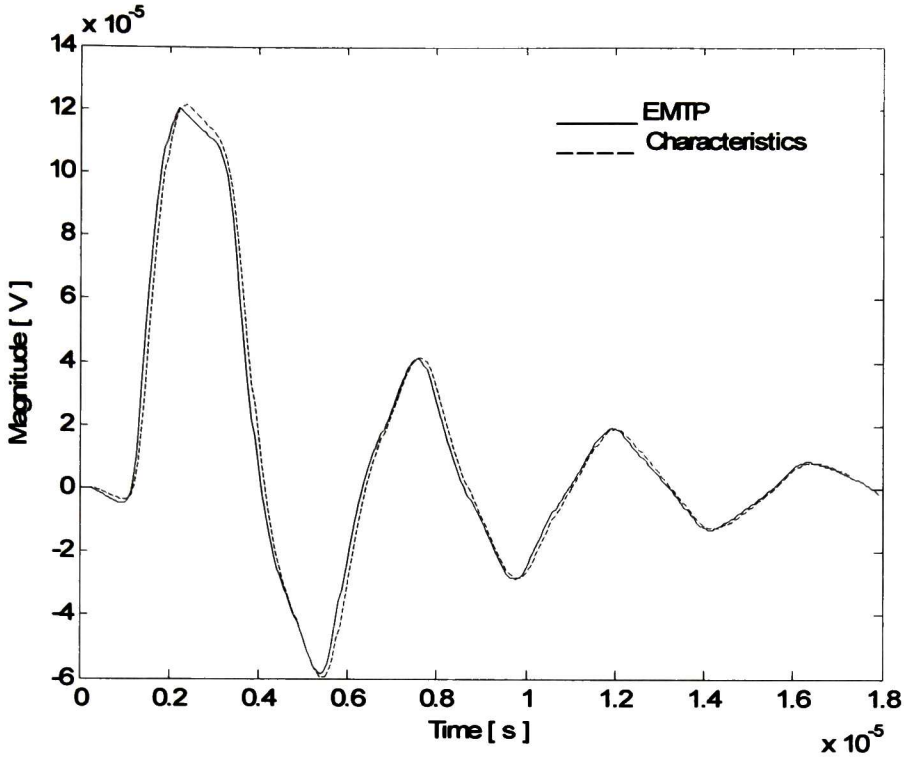

Fig.5.9. Voltage waveforms at the sending end (and receiving end) for the EMTP and the Method of Characteristics.

5.6 OBSERVATIONS

In this Chapter the method of Characteristics has been applied to the analysis of electromagnetic transients in nonuniform multiconductor transmission lines illuminated by incident electromagnetic plane waves. The proposed method does not present numerical oscillations which are very common in finite difference procedures. The results obtained with the method of characteristics showed good agreement with those from the EMTP. Results from the EMTP do not present numerical oscillations, however, this simulation method is very cumbersome and the accuracy of the results depends on the expertise of the user.

6 Conclusions And Future Work

6.1 Conclusions

In this work the Method of Characteristics has been applied to the analysis of electromagnetic transients in NU multiconductor TLs with frequency dependent electrical parameters. To solve the TL equations a time domain modal analysis that yields real eigenvalues and eigenvectors has been performed. To include the frequency dependence of the electrical parameters the convolution operation has been simplified by using the vector fitting technique. In addition Norton models for the TL ends have been developed in order to make the method suitable to be included into general-purpose programs.

As can be seen from the results the method of Characteristics yields almost the same results as the EMTP and NLTP. It should be noticed the practical difficulty involved when using the EMTP or NLTP. With both methods the transmission line has to be divided in several segments and each one must be included as a uniform transmission line by itself. For a particular simulation the user has to decide about the number of segments based on his expertise. When a new simulation with a different number of segments is required, the electrical parameters have to be calculated again and a new data file (or network) has to be created. This procedure in practice can be very cumbersome and lengthy for the user.

The proposed model can be applied to any geometrical configuration and does not require damping techniques. Therefore it could help to determine whether the oscillations, or the lack of them, presented in a time domain analysis are part of the transient phenomenon or due to numerical errors.

The Nonuniform transmission line model has been simplified and a piece-wise uniform line model has been developed. This model does not require the spatial derivatives of the transformation matrices, therefore provides computer time savings. In spite of being a simplified model it yields very good results and removes the possibility of numerical oscillations inherent to the numerical approximation of the transformation matrices derivatives.

Finally two procedures for calculating electromagnetic transients in field excited nonuniform multiconductor transmission lines have been presented. The first one is based on the Finite Difference Time Domain method or Yee's Method and the second one is an extension of the model based on the Method of Characteristics.

The Finite Difference Time Domain model presented numerical oscillations in the case of independent excitations applied at the transmission line ends but it yielded correct results for field excited transmission lines (without independent sources).

The model based in the method of characteristics (piecewise uniform) proved to be robust and provide correct results for any kind of excitation.

6.2 Future Work

Finally, with the model proposed for nonuniform lines there are several possibilities for future works as follows:

1) Extension of the piece-wise transmission line model to a number of practical cases, such as: towers, transformers and electrical machines.
2) Using the same idea of the piece-wise uniform model a piece-wise linear model can be develop for the case of nonlinear phenomena (corona effect for example)
3) Inclusion of the proposed model in a commercial program, such as the ATP or the Power System Toolbox of Matlab.

REFERENCES

[1] C. F. Wagner, I. W. Gross y B. L. Lloyd, "High-Voltage Impulse Tests on Transmission Lines" AIEE Winter General Meeting, New York, N. Y. January 28-22, 1954.

[2] C. Menemenlis and Z. T. Chun, "Wave Propagation on Nonuniform Lines", IEEE Trans. Power Apparatus and Systems, vol. PAS-101,no.4,pp.833-839,April 1982.

[3] A. Ametani y M. Aoki, "Line Parameters and Transients of a Non-Parallel Conductors System", IEEE Trans. Power Delivery, vol. 4, no.2, April 1989.

[4] M. M. Saied, A. S. Alfuhaid y M. E. El.-Shandwily, "S-Domain Analysis of Electromagnetic Transients on Nonuniform Lines", IEEE/PES 1998, Summer Meeting Portland Oregon, Julio 24-29, 1988.

[5] M. T. Correia de Barros y M. E. Almeida, "Computation of Electromagnetic Transients on Nonuniform Transmission Lines", IEEE Trans. Power Delivery vol. 11, no.2, April 1996.

[6] H. V. Nguyen, H. W. Dommel y J. R. Marti, "Modelling of Single-Phase Nonuniform Transmission Lines in Electromagnetic Transient Simulations", IEEE Trans. Power Delivery, vol.12, no.2, April 1997.

[7] A. Semlyen, "Some Frequency Domain Aspects of Wave Propagation on Nonuniform Lines", IEEE Trans. Power Delivery, vol.18, no.1, January 2003.

[8] J. A. Gutierrez, J. L. Naredo, L. Guardado, and P. Moreno, "Transient Analysis of Nonuniform Transmission Lines through the Method of Characteristics", Proc. of the ISH-99, 11th International Symposium on High Voltage Engineering, vol. 2, topic B, London, U. K., August 23-27, 1999.

[9] M. Davila, J. L. Naredo and P. Moreno, "Transient Analysis of Power Lines Including Non Uniform and Frequency Dependent Effects", North American Power Symposium (NAPS) 2002, Tempe, Arizona, U.S.A., October 2002.

[10] M. S. Mamis y M. KöKsal, "Lightning Surge Analysis Using Nouniform Single-Phase Line Model", IEE Proc. Gener., Transm., Distrib.,vol.148 no.1, January 2001.

[11] A. I. Ramirez, A. Semlyen y Reza Iravani, "Modelling Non-Uniform Transmission Lines for Time Domain Simulation of Electromagnetic Transients", IEEE Trans. Power Delivery.

[12] Clayton R. P. "Frequency Response of Multiconductor Transmission Lines Illuminated by an Electromagnetic Field", IEEE Trans. on Electromagnetic Compatibility, vol. EMC-18,no. 4, November 1976.

[13] A. K. Agrawal, H. J. Price y S. H. Gurbaxani, "Transient Response of Multiconductor Transmission Lines Excited by a Nonuniform Electromagnetic Field", IEEE Trans. on Electromagnetic Compatibility, vol.EMC-22,no.2,May 1980.

[14] T. Henriksen, "Calculation of Lightning Over Voltages Using EMTP", IPST'95, International Conference on Power Systems Transients Lisboan, 3-7 September 1995.

[15] A. Xemard, Ph. Baraton y F. Boutet, "Modelling with EMTP of Overhead Lines Illuminated by an External Electromagnetic Field", IPST'95, International Conference on Power Systems Transients Lisbon,3-7 September 1995.

[16] M. D'Amore y M. S. Sarto, "An EMTP-Compatible Procedure For The Evaluation Of Electromagnetic Induced Effects On Power Networks", IPST'95, International Conference on Power Systems Transients, Lisbon, 3-7 September 1995.

[17] E. A. Oufi, A. S. Al-Fuhaid, M. M. Saied, "Transient Analysis of Lossless Single-phase Nonuniform Transmission Lines", IEEE trans PWRD, vol. 9, No.3, pp.1694-1700, 1994.

[18] J. L. Naredo, "The Effect of Corona on Wave Propagation on Transmission lines" Ph.D. Thesis, Department of Electrical Engineering Faculty of Applied Science, The University of British Columbia, 1992.

[19]. J.A. Gutiérrez, P. Moreno, J.L. Naredo, J.C. Gutiérrez, "Fast Transient analysis of nonuniform lines through the method of characteristics", International Journal of Electrical Power and Energy Systems, Vol.24, No.9, pp. 781-788, Oct. 2002.

[20].-J. A. Gutiérrez R., P. Moreno, J. L. Naredo, J. L. Bermúdez, M. Paolone, C. A. Nucci, and F. Rachidi, "Nonuniform Transmission Tower Model for Lightning Transient Studies", IEEE Trans. Power Delivery, vol. 19, No. 2, pp. 490-496, April 2004.

[21].- Abner Ramírez, José L. Naredo, Pablo Moreno, Leonardo Guardado, "Electromagnetic Transients in overhead lines considering frequency dependence and corona effect via the method of characteristics", Int. J. Of Electrical Power and Energy Systems, Vol. 23, No. 3, pp. 179-188, February 2001.

[22] Abner Ramirez, J. Luis Naredo, Pablo Moreno, "Full Frequency-Dependent Line Model for Electromagnetic Transient Simulation Including Lumped and Distributed Sources", IEEE Trans. Power Delivery, vol. 20, No. 1, pp. 292-299, January 2005.

[23] P. Moreno, R. de la Rosa, J.L. Naredo, "Frequency Domain Computation of Transmission Line Closing transients", IEEE Trans. on Power Delivery, Vol.6, No.3, 1991.

[24] R. Radulet, Al. Timotin, A. Tugulea, A. Nica, "The Transient Response of the Electric lines Based on the Equations with Transient Lines Parameter", Rev. Roum. Sci. Techn., vol. 23, o. 1 ,pp. 3-19, 1978.

[25] R. H. Galloway, W. B. Shorrocks and L. M. Wedepohl, "Calculation of Electrical Parameters for Short and Long Polyphase Transmission Lines", Proc. IEE, Vol. 111, pp. 2051-2059, Dec. 1964.

[26] A. Deri, G. Tevan, A. Semlyen and A. Castanheira, "The complex Ground Return Plane: A Simplified Model for Homogeneous and Multi-layer Earth Return" IEEE Trans. Power Apparatus and Systems, vol. PAS-100 no. 8,pp. 3686-3693, August 1981.

[27] M. E. Van Valkenburg, "Introduction to Modern Network Synthesis", John Wiley & Sons, Inc., 1960.

[28] J. R. Marti, "Accurate Modelling of Frequency-Dependent Transmission Lines in Electromagnetic Transient Simulations", IEEE Trans. Power Apparatus and Systems, vol. PAS-101,No.1, January 1982.

[29] L. Silveira, M. Elfadel, J. White, M. Chilukuri and K. Kundert, "Efficient Frequency-Domain Modeling and Circuit Simulation of Transmission Lines", IEEE Transactions on Components, Packaging and Manufacturing Technology-Part B, Vol. 17, No. 4, pp. 505-513, November 1994.

[30] D. B. Kuznetsov and J. E. Schutt-Ainé, "Optimal Transient Simulation of Transmission Lines", IEEE Transactions on Circuits and Systems-I: Fundamental Theory and Applications, Vol. 43, No. 2, pp. 110-121, February 1996.

[31]. B. Gustavsen and A. Semlyen. "Combined Phase Domain and Modal Domain Calculation of Transmission Line Transients Based on Vector Fitting", IEEE Trans. Power Delivery, vol. 13, no.2, pp. 596-604, April 1998.

[32].-L. M. Wedepohl, "Application of Matrix Methods to the solution of travelling wave phenomena in polyphase systems", Proc. IEE, Vol. 110, No.12, pp. 2200-2212, December 1963.

[33].-J. C. Strikwerda, "Finite Differences Schemes and Partial Differential Equations", Mathematics Series, Pacific Grove: Wadsworth, 1989.

[34].-Juan Carlos Gutierrez Villegas, "Modelado de Líneas de Transmisión Monofásicas con Parámetros dependientes de la distancia y Condiciones Arbitrarias en los extremos para el Análisis de Transitorios Electromagnéticos", Master of Science in Electrical Engineering thesis, CINVESTAV Unidad Guadalajara octubre 2000.

[35] Mattew N. O. Sadiku, "Numerical Techniques in Electromagnetics", Crs Press Boca Raton ann arbor London Tokyo.

[36] Clayton R. Paul "Analysis of Multiconductor Transmission Lines", Department of Electrical Engineering, University of Kentucky, A Wiley-Interscience Publication, 1994.

PUBLISHED WORK

[1]. Pablo Moreno, Alejandro. R. Chávez B., José L. Naredo, Leonardo Guardado, "Fast Transients Análisis of Non-Uniform Multiconductor Transmisión Lines", IEEE/PES Transmission and Distribution 2002 Latin America, Sao Paulo, Brasil, March 18-22, 2002.

[2]. Alejandro R. Chávez B., Pablo Moreno V., José L. Naredo, "Fast Transients Analysis of Non-uniform Multiconductor Transmission Lines Excited by Incident Field", IEEE Bologna Power Tech, June 23-26, 2003, Bologna Italia.

[3]. A.R. Chávez, P. Moreno, J.L. Naredo, L. Guardado, "Fast transients analysis of Non-uniform multiconductor frequency-dependent transmission lines", *IEEE Transactions on Power Delivery*, vol.21, no.2, pp. 809-815, April 2006.

CENTRO DE INVESTIGACIÓN Y DE ESTUDIOS AVANZADOS DEL I.P.N.
UNIDAD GUADALAJARA

El Jurado designado por la Unidad Guadalajara del Centro de Investigación y de Estudios Avanzados del Instituto Politécnico Nacional aprobó la tesis

Nonuniform Multiconductor Transmission Lines Modeling for Time Domain Electromagnetic Transient Studies

del (la) C.

Alejandro Rafael CHÁVEZ BUSTOS

el día 19 de Octubre de 2007.

Dr. Pablo Moreno Villalobos
Investigador CINVESTAV 3C
CINVESTAV Unidad Guadalajara

Dr. José Luis Naredo Villagrán
Investigador CINVESTAV 3C
CINVESTAV Unidad Guadalajara

Dr. Amner Israel Ramírez Vázquez
Investigador CINVESTAV 3A
CINVESTAV Unidad Guadalajara

Dr. José Raúl Loo Yau
Investigador CINVESTAV 2B
CINVESTAV

Dr. José Leonardo Guardado Zavala
Profesor Investigador Titular C
Instituto Tecnológico de Morelia